Properties of lightly doped t-J two-leg ladders

Matthias Troyer[a,b,*], Hirokazu Tsunetsugu[a,b,c], and T. M. Rice[b]
[a] *Interdisziplinäres Projektzentrum für Supercomputing, Eidgenössische Technische Hochschule, CH-8092 Zürich, Switzerland*
[b] *Theoretische Physik, Eidgenössische Technische Hochschule, CH-8093 Zürich, Switzerland*
[c] *Institute of Applied Physics, University of Tsukuba, Tsukuba, Ibaraki 305, Japan*
(Received)

arXiv:cond-mat/9510150v1 26 Oct 1995

We have numerically investigated the doped t-J ladder using exact diagonalization. We have studied both the limit of strong inter-chain coupling and isotropic coupling. The ladder scales to the Luther-Emery liquid regime in the strong inter-chain coupling limit. In this strong coupling limit there is a simple picture of the excitation spectrum that can be continued to explain the behavior at isotropic coupling. At $J = 0$ we have indications of a ferromagnetic ground state. At a large J/t the ladder is phase separated into holes and a Heisenberg ladder. At intermediate coupling the ground state shows hole pairing with a modified d-wave symmetry. The excitation spectrum separates into a limited number of quasiparticles which carry charge $+|e|$ and spin $\frac{1}{2}$ and a triplet magnon mode. At half-filling the former vanish but the latter evolves continuously into the magnon band of the spin liquid. At low doping the quasiparticles form a dilute Fermi gas with a strong attraction but simultaneously the Fermi wave vector, as would be measured in photoemission, is large. The dynamical structure factors are calculated and are found to be very similar to calculations on 2D clusters.

PACS numbers: 74.20.Mn, 71.27.+a, 74.25.Ha

I. INTRODUCTION

The properties of strongly correlated electrons confined to a ladder (or double chain) and described by t-J or Hubbard models have been the subject of intensive investigation recently.[1–7] The reason lies in the unusual spin liquid nature of the undoped parent system.[1,8–14] Another reason for especial interest is weakly coupled ladders compounds like $SrCu_2O_3$ and $(VO)_2P_2O_7$.[15,16] Recent measurements of the magnetic susceptibility and the nuclear spin relaxation rate in these materials show the existence of a finite spin gap.

The key question in the current study is the evolution of the finite gap in the spin excitation spectrum upon doping. The spin gap remains in other spin liquids systems and is a sign of strong superconducting fluctuations.[17,18]

A recent analysis of the t-J ladder using a mean-field theory with Gutzwiller renormalization of the matrix elements to account for the strong correlations, gave a continuous evolution of the spin gap with doping.[5] The short range resonance valence bond (RVB) state evolves into a superconductor with modified d-wave symmetry within this mean-field approximation. A tendency towards modified d-wave superconductivity was also found in a bosonization approach[6] and in a recent numerical study of the Hubbard ladder.[2]

We have investigated t-J ladders up to a size of 10×2 sites using a Lanczos diagonalization method. First results have been published in Ref. 3. Here we report in more detail our results for larger lattices including a detailed investigation of the excitation spectrum, a discussion of phase separation and the calculation of the superconducting order parameter and of the form factor of the Cooper pairs.

We find clear evidence of hole pairing and a modified d-wave RVB state in lightly doped systems in agreement with the mean-field theory. An interesting difference however is the discontinuous evolution of the excitation spectrum upon doping. New "quasiparticle" excitations appear carrying both charge and spin. These excitations are in addition to a band of magnons which evolve continuously away from the undoped spin liquid. This separation of the excitation spectrum into bound holon-spinon quasiparticles and collective magnon excitation contrasts with the full spin-charge separation found in a Luttinger liquid.

The t-J ladder Hamiltonian is

$$\begin{aligned}\mathcal{H} = &-t \sum_{j,\sigma,a} \mathcal{P} \left(c^\dagger_{j,a,\sigma} c_{j+1,a,\sigma} + \text{H.c.} \right) \mathcal{P} \\ &-t' \sum_{j,\sigma} \mathcal{P} \left(c^\dagger_{j,1,\sigma} c_{j,2,\sigma} + \text{H.c.} \right) \mathcal{P} \\ &+J \sum_{j,a} \left(\mathbf{S}_{j,a} \cdot \mathbf{S}_{j+1,a} - \tfrac{1}{4} n_{j,a} n_{j+1,a} \right) \\ &+J' \sum_{j} \left(\mathbf{S}_{j,1} \cdot \mathbf{S}_{j,2} - \tfrac{1}{4} n_{j,1} n_{j,2} \right),\end{aligned} \tag{1}$$

where j runs over L rungs, and σ ($=\uparrow,\downarrow$) and a ($=1,2$) are spin and leg indices. The t-J ladder is sketched in Fig. 1. The first two terms are the kinetic energies and the J (J') are exchange couplings along the ladder (rungs). Unless noted otherwise we set $t' = t$. The projection operator $\mathcal{P} \equiv \prod_{i,a}(1 - n_{i,a,\uparrow} n_{i,a,\downarrow})$ prohibits double occupancy of a site. Periodic or antiperiodic boundary conditions (PBC, APBC) are used along the ladder. The wave vector $\mathbf{k} = (k_x, k_y)$ is consequently well defined, k_x and k_y being the momenta along the ladder and rungs.

The transverse momentum k_y takes only the values 0 and π, corresponding to bonding and antibonding states.

At half filling the t-J ladder is equivalent to the Heisenberg ladder, which was investigated in earlier publications.[1,5,10–14] The ground state of the Heisenberg ladder is a short range RVB state with a spin gap of $\Delta \approx J/2$[1,11,13,14] at isotropic coupling, $J' = J$.

The strong coupling limit $J'/J \to \infty$ is a good starting point to describe the system as there a simple description of the spectrum is available.[19] In that limit, each eigenfunction of the total system can be written as a direct product of one-rung states, which are either spin singlets or one of the triplets, and the ground state is that with all singlets. The first excited multiplet consists of the states with one triplet rung. A small but finite value of J lifts the degeneracy of these states. The one-magnon excitations then form a three-fold spin degenerate band with dispersion $\epsilon_k = J' + J\cos k_x + \frac{1}{4}(J^2/J')(3 - 2\cos 2k_x)$ up to second order in J. It has a minimum gap $\Delta = J' - J + \frac{1}{2}\frac{J^2}{J'}$ at $k_x = \pi$.[19] The momentum perpendicular to the chains is $k_y = \pi$. The higher excited states form a continuum of excited states and its minimum is at $\mathbf{k} = (0, 0)$ with energies slightly larger than twice the gap 2Δ. With increasing J the collective excitation branch crosses into the continuum, but the qualitative description is still valid.

In this paper we study the effects of doping holes into such a ladder. Although the isotropic case, $J'/J = 1$, is of most interest, we also study the limit $J' \gg J, t$, which can be easily understood. In this limit the problem reduces to a system of weakly coupled rungs. The properties can be continuously followed down to the isotropic point $J = J'$.

This paper is organized as follows. In Sec. II we briefly discuss the occurrence of ferromagnetism in the ladder doped with one or two holes at $J = 0$ and discuss the relationship with the occurrence of ferromagnetism in two dimensions. Next in Sec. III we discuss the pairing of holes doped into the ladder and the occurrence of phase separation. To understand the excitation spectra we start from the single hole case in Sec. IV and go on to the two-hole case in Sec. V. Section VI discusses long range correlations, in particular the interesting question of the symmetry of the pairs and the mapping to a Luther-Emery liquid. The single-particle excitations are discussed in Sec. VII. Over all we find a remarkable similarity between the ladder and 2D clusters.

II. FERROMAGNETISM FOR $J = 0$

The t-model (t-J model with $J = 0$) is equivalent to the infinite-U Hubbard model. In single chains the ground state of the t-model is degenerate in the spin degrees of freedom. In two dimensions on the other hand the ground state of the t-model doped with one hole is ferromagnetic.[20] This is called the Nagaoka effect.

The extension of the proof by Nagaoka to finite hole doping in the thermodynamic limit proved to be difficult. Actually the ground state of the two-dimensional (2D) square-lattice t-model doped with *two* holes is *not* ferromagnetic.[21] For finite densities in the thermodynamic limit there are contradicting results. Variational estimates for the $U = \infty$ Hubbard model indicate that the fully polarized ferromagnetic state is stable until a critical doping $\delta_{cr} = 0.29$.[22] High temperature series expansions by Putikka *et al.* on the other hand show evidence that the fully polarized ferromagnetic ground state does not survive at any finite doping. Instead they find evidence for a partially polarized ferromagnetic state at low hole doping. A fully polarized ferromagnetic state at finite doping was found only for $J < 0$.[23]

In this context it is of interest to study the occurrence of ferromagnetism in the ladder models. While the proof by Nagaoka[20] cannot be applied to the one-dimensional chain it is valid for the ladder. The proof relies on the existence of closed loops on the lattice. Such loops exist in 2D lattices and on ladders, but cannot be formed on single chains. The ground state of the ladder doped with one hole is thus ferromagnetic.

We have numerically studied the t-ladder with $L = 2, 3, \ldots, 10$ rungs, doped with two holes. In Fig. 2 we show the ground state energies of the ladders for both PBC's and APBC's. We find that the ground state is always ferromagnetic for APBC and an even number of rungs and for PBC and an odd number of rungs. For the other boundary conditions the ground state is a spin singlet.

An important point is that the ferromagnetic state always has the lower energy for a ladder with at least four rungs. The singlet state is very close in energy and deserves a more detailed investigation. In Fig. 3 we plot the real-space spin correlations $\langle S^z(0)S^z(r)\rangle$ of the lowest singlet state of the $L = 10$ ladder. These spin correlations show that the singlet state actually consists of two ferromagnetic domains with opposite magnetization.

The results show clear evidence for a ferromagnetic ground state of the t-ladder ($L \geq 4$) doped with two holes. In the thermodynamic limit however two holes is not a finite density. Extrapolations of our small-cluster results at finite doping to the thermodynamic limit $L \to \infty$ are hard to obtain. But one may speculate that the existence of a ferromagnetic ground state of the t-ladder with 2 holes and $L \geq 4$ could indicate a ferromagnetic state for dopings $\delta < \delta_{\rm cr} \approx 0.25$. Similar results were obtained by Hirsch and Müller-Hartmann.[24]

III. HOLE PAIRING AND PHASE SEPARATION

A. Hole Pairing

In this section we will discuss the pairing of holes doped into the t-J ladder and the occurrence of phase separation at large values of J/t. We will start from the simple limit

$J' \gg J, t$. In this limit the undoped ladder consists of weakly coupled rungs, as is sketched in Fig. 4(a).

In this limit two holes doped into the ladder will go onto the same rung in order to minimize the number of broken singlet bonds. This state is graphically shown in Fig. 4(c). In order to study the occurrence of hole pairing at smaller values of J' and down to the isotropic point $J = J'$ we calculate the binding energy and the hole-hole correlation function. We find that even at isotropic coupling the holes still form a bound pair, although the pair is more spread out there.

The binding energy E_B is defined as

$$E_B \equiv 2E_{\mathrm{G.S.}}(2L-1) - E_{\mathrm{G.S.}}(2L) - E_{\mathrm{G.S.}}(2L-2), \quad (2)$$

where $E_{\mathrm{G.S.}}(N)$ is the ground state energy for N electrons, the boundary conditions are chosen between PBC and APBC to give the lowest energy.

In the large J' region the binding energy can easily be estimated. A single hole doped into a Heisenberg ladder breaks one bond with energy loss J', but can gain kinetic energy $-t$ along the ladder (see the next section for details) and $-t'$ along the rung. It follows that $E_{\mathrm{G.S.}}(2L-1) \approx E_{\mathrm{G.S.}}(2L) + J' - t - t'$. Two holes on the same rung also break one bond, but the kinetic energy of such a bound pair is much smaller, of order $-4t^2/J'$, as will be calculated later. Thus we estimate $E_{\mathrm{G.S.}}(2L-2) \approx E_{\mathrm{G.S.}}(2L) + J'$, and a binding energy:

$$E_B \approx J' - 2t - 2t' \qquad \text{for } J' \gg J, t, t' \ . \quad (3)$$

Figure 5 shows E_B as a function of J'. It remains positive and thus shows binding down to the isotropic value, $J/t = J'/t = 0.3$. The same holds for a larger $J/t = 0.5$.

Additional evidence for pairing is provided by the hole-hole correlation functions

$$\langle n_{\mathrm{h}}(0) n_{\mathrm{h}}(r) \rangle \equiv \langle (1-n_{i,a})(1-n_{i+r,a'}) \rangle, \quad (4)$$

measured on the same leg $a = a'$ and on different legs $a \neq a'$ in the ground state. They are plotted in Fig. 6 for $J/t = 0.3$ and $J'/J = 1$ and 10. For $J'/J \gg 1$ the two holes are predominantly on the same rung and the correlation function shows a clear exponential decay. At the isotropic point the pair is more extended. The maximum of the correlation function is now at a distance 1 along the legs and on different legs, but it again decays at large distances. We can calculate the size of the hole pair by fitting the inter-chain correlations to an exponential form $\langle n_{\mathrm{h}}(0) n_{\mathrm{h}}(r) \rangle \sim e^{-r/\xi} + e^{-(L-r)/\xi}$ for the two largest distances, $L/2$ and $L/2-1$. The inset of Fig. 6 shows the size ξ of the hole pair as a function of the inter-chain coupling J'/t. The pair is very tightly bound for $J' \gg J$. At the isotropic point the pair is still bound, with a diameter of about two lattice spacings. Note the oscillation of the radius with respect to L. The size seems to converge to a value in between the $L = 8$ and the $L = 10$ result at the isotropic point.

B. Effective boson model for the large J' limit

We may say that the system belongs to the Luther-Emery universality class of 1D correlated systems,[25] in the sense that the spin excitations acquire a finite gap while the charge excitations remain gapless. In the limit of large J', however, the picture that tightly bound hole pairs are moving in a background of singlet rungs is more appropriate than weak coupling approaches like g-ology. Considering these hole pairs as hard core bosons, we can determine the long-range correlations by a mapping to an effective boson model.

The pair hopping matrix element to second order in perturbation theory is

$$t^* = \frac{2t^2}{J' - 4t'^2/J'}. \quad (5)$$

There is a weak attraction V^* between two hole pairs on neighboring rungs, which again to second order takes the form

$$V^* \equiv -\frac{J}{2} - \frac{3J^2}{8J'} + \frac{4t^2}{J' - 4t'^2/J'}, \quad (6)$$

where the first, attractive, term comes from the charge part of the J-term in the Hamiltonian. As $t^*, V^* \ll J'$ we can map the low-energy part of the t-J ladder onto an effective hard-core boson model on a chain with nearest neighbor interaction:

$$H^* = -t^* \sum_i \left(B_i^\dagger B_{i+1} + \text{H. c.} \right) + V^* \sum_i N_i N_{i+1}, \quad (7)$$

where the hard-core boson creation operator $B_i^\dagger$ creates a hole pair at the rung i and $N_i \equiv B_i^\dagger B_i$ is its number operator. There is a hard-core repulsion since only one hole pair can be created on any given rung.

Our effective boson model is equivalent to the XXZ-model in a magnetic field, which has been solved exactly by a bosonization approach and conformal field theory.[26] For $V^* < -2|t^*|$ the system is phase separated. This is the case for $J' > J'_{\mathrm{PS}}$, where

$$J'_{\mathrm{PS}} = \frac{16\, t^2}{J} - \frac{J}{2} + \mathrm{O}\left(\frac{J^3}{t^2}\right), \quad (8)$$

again to second order perturbation theory. For physically reasonable values of J/t phase separation occurs only at very large values of J': $J'_{\mathrm{PS}}/t = 53.2$ for $J/t = 0.3$ and $J'_{\mathrm{PS}}/t = 31.8$ for $J/t = 0.5$. Note that the dominant attractive part of the interaction comes from the charge part $-\frac{1}{4} J n_{j,a} n_{j+1,a}$ of the J-term.

Next we will discuss the region where the system is not yet phase separated but J' is still large ($J, t \ll J' < J'_{PS}$). There we can determine the dominant correlations from the effective boson model. The correlation exponents have been calculated indirectly by Bethe ansatz.[26] Both

the charge density wave correlations and the superconducting correlations show a power-law decay at large distances:

$$\langle N_r N_0 \rangle \sim \text{const.} \times r^{-2} + \text{const.} \times \cos\bigl(2k_F r\bigr)\, r^{-K_\rho}, \quad \text{(9a)}$$

$$\langle B_r^\dagger B_0 \rangle \sim r^{-1/K_\rho}. \quad \text{(9b)}$$

The superconducting correlations $\langle B_r^\dagger B_0 \rangle$ are dominant if $K_\rho > 1$. This is the case for most of the phase diagram, except for the phase separation regime at $V^* < -2t^*$. At quarter filling $\rho = 1/2$ and for $V^* > 2t^*$ the system is in the Ising-limit and shows a long range charge density wave ground state. At fillings close to that line and for large $V^* > 2t^*$ there is a small region where $K_\rho < 1$.[26]

In our effective model we have $V^* < 0$ and there $K_\rho > 2$.[26] We are thus always in the region of dominant superconducting correlations. Even neglecting the attractive charge part of the J-term we are still in the superconducting regime where $K_\rho > 1$.

In the limit of large J' the equivalence of the t-J ladder with a Luther-Emery liquid can clearly be seen. Going to isotropic coupling the spin gap remains finite and the only low-lying excitation is the collective charge mode, as we will show in the following sections. Thus also at isotropic coupling the t-J ladder is still a Luther-Emery liquid. In Sec. VI B, we will develop another approach which relates the long-range correlations to thermodynamic quantities for more general J's, based on a bosonization of density fluctuations.

C. Phase separation

Finally we study the occurrence of phase separation at isotropic coupling $J = J'$. We estimate the onset of phase separation by determining the coupling J at which the compressibility κ diverges. The compressibility per site can be calculated as usual

$$\kappa^{-1} = \rho^2 \, \frac{\partial^2 \epsilon(\rho)}{\partial \rho^2} \,, \quad (10)$$

where $\epsilon(\rho)$ is the energy density per site of the ladder with a particle density per site $\rho = N/(2L)$.

In a finite system usually the discrete version

$$\kappa^{-1} = \frac{N^2}{2L} \left[\frac{E(N+2;L) + E(N-2;L) - 2E(N;L)}{4} \right] \quad (11)$$

is used, where $E(N;L)$ is the ground state energy of the finite system with N particles on the ladder with L rungs (Volume $2L$). At small hole doping however this procedure may not be reliable due to finite size effects caused by frustration on small lattices. To see this let us consider the $L = 8$ ladder doped with zero, two or four holes. In the undoped case there are 8 spins on each leg of the ladder. Two holes doped into the ladder will predominantly go onto different legs and there will be seven spins per leg. Thus the antiferromagnetic configuration on the legs will be frustrated. For four holes there will be six holes on each leg and the system is again not frustrated. Conversely on an $L = 9$ ladder the undoped ladder and the ladder doped with four holes will be frustrated, while the ladder doped with two holes will be non-frustrated.

We have thus used a different formula to calculate the compressibility at small hole doping. We calculate the ground state energies for an $L = 8$ ladder doped with $N_\mathrm{h} = 0$ and 4 holes and for an $L = 9$ ladder doped with 2 and 6 holes. In all these cases the ladder is not frustrated. Then we estimate the compressibility from these energies using finite differences similar to the above Eq. (11). In the thermodynamic limit $L \to \infty$ both formulas give the same result, as the frustration appears only on small lattices.

While the finite size effects are quite small at low electron densities they are much larger at small hole dopings due to frustration mentioned before. The estimated errors on the phase separation line may thus be much larger there, about $\pm 0.2t$.

A comparison with the results obtained with open boundary conditions (OBC) confirms our results. Only at small doping the OBC results are not reliable since there the holes are trapped on the ends of the chain.

Figure 7 shows the phase separation line for the t-J ladder for $J = J'$, in the J-ρ plane. Note that, opposite to the single chain case,[27] the onset of phase separation at small hole doping is at lower values of J/t than at small electron concentrations. This resembles the behavior in two dimensions,[23] although the precise position of the phase separation line in two dimensions has not yet been established.

IV. PROPERTIES OF A SINGLE HOLE

In the previous section we have discussed the ground state of the ladder doped with two holes. In order to understand the low energy excitations of the ladder it is useful to study the one-hole problem first.

As mentioned above the limit $J' \gg J, t$ is a good starting point to explore the t-J ladder. There are nine different states, depicted in Fig. 8. A single electron goes either into the bonding or antibonding orbital

$$b_{i,\sigma}^\dagger = \frac{1}{\sqrt{2}} \left(c_{i,1,\sigma}^\dagger + c_{i,2,\sigma}^\dagger \right), a_{i,\sigma}^\dagger = \frac{1}{\sqrt{2}} \left(c_{i,1,\sigma}^\dagger - c_{i,2,\sigma}^\dagger \right), \quad (12)$$

with energy $\mp t'$, respectively. Two electrons on the rung are either in the singlet state with energy $-J'$ or in one of the three triplet states with energy 0. The singlet state expressed in bonding and antibonding orbitals is

$$\frac{1}{\sqrt{2}}\left(c^\dagger_{i,1,\uparrow}c^\dagger_{i,2,\downarrow}-c^\dagger_{i,1,\downarrow}c^\dagger_{i,2,\uparrow}\right)=\frac{1}{\sqrt{2}}\left(b^\dagger_{i,\uparrow}b^\dagger_{i,\downarrow}-a^\dagger_{i,\uparrow}a^\dagger_{i,\downarrow}\right) \tag{13}$$

Similarly the three triplets can be expressed as combinations of one bonding and one antibonding electron:

$$a^\dagger_\uparrow b^\dagger_\uparrow,\ \frac{1}{\sqrt{2}}\left(a^\dagger_\uparrow b^\dagger_\downarrow+a^\dagger_\downarrow b^\dagger_\uparrow\right),\ a^\dagger_\downarrow b^\dagger_\downarrow \tag{14}$$

Figures 9(a) and (b) show the one-hole spectra for $L = 8$ for large inter-chain coupling $J'/J = 10$, calculated by exact diagonalization for $J/t = 0.3$, $J'/t = 3$ and $J/t = 0.5$, $J'/t = 5$ respectively.

A hole on a single rung can be either in the bonding or the antibonding orbital. One hole doped into the half filled ladder will thus be either in a bonding or antibonding state, depending on the parity symmetry of the total ladder [see Fig. 4(b)]. This hole can propagate along the ladder with a hopping matrix element $\tilde{t} = +t/2$ in first order perturbation theory. Thus the low energy states are two bands of holes in the bonding and anti-bonding orbitals. They are split by the energy difference $2t'$ of the bonding and antibonding states. These two bands can clearly be seen in the spectra [Figs. 9(a) and (b)]. The minimum of the bands is at $k_x = \pi$, since the hopping matrix element for holes $\tilde{t} > 0$. The bandwidth of both bands is $4\tilde{t} = 2t$ in the limit $J' \gg J, t$. At finite J the bandwidth is reduced due to hybridization with the higher excited states.

Decreasing J' to the isotropic points $J = J'$ changes the dispersion of these bands [see Figs. 9(c) and (d)]. At low energies we can still see the bands of holes in the bonding and antibonding orbitals. These bands evolve continuously from the large J' limit. The minima of the energy bands are not at $k_x = 0$ or $k_x = \pi$, but at a large momentum $\mathbf{k}^B_F \approx \left(\pm\frac{3}{5}\pi, 0\right)$ for the bonding and $\mathbf{k}^A_F \approx \left(\pm\frac{2}{5}\pi, \pi\right)$ for the antibonding band. We can fit the low-lying hole bands to a dispersion of the form

$$E(k_x) = E_0 + \Delta E + \alpha_1 \cos k_x + \alpha_2 \cos 2k_x + \alpha_3 \cos 3k_x, \tag{15}$$

corresponding to nearest neighbor (α_1), next-nearest neighbor (α_2) and third-nearest neighbor (α_3) hopping. E_0 is the ground state energy of the undoped ladder and ΔE the shift in energy of the center of the band upon doping. In Fig. 10 we show the bands and the excellent fit. The parameters are shown in Table I.

The changes in the hole dispersion with decreasing J' are summarized as follows:

(i) The center of the bands shifts downwards by $\Delta E < 0$, compared to the undoped ladder. The energy gain for one hole in the case of $J = 0$ would be just the kinetic energy $-t'$. When $J > 0$ we lose magnetic energy by introducing the hole. The energy gain is therefore smaller at larger J/t, as we can also see from the fit parameters.

(ii) The hole bands are narrowed compared to the large J' limit. In that limit the bandwidth of the hole bands was $2t$. This bandwidth is renormalized by the stronger polarization effects at isotropic coupling, and it is now of the same order as the magnetic energy J, instead of the kinetic energy $2t$.

(iii) The dispersion changes as longer range hopping processes (α_2, α_3) are introduced with decreasing J', and the minima move away from $k_x = \pi$. The minima of both bands are very close in energy, again in contrast to the strong coupling region where they are split by $2t'$. In Sec. VII we will identify the minima k^B_F and k^A_F with the Fermi points of the bonding and antibonding quasiparticle bands.

Another interesting question is the behavior of the free spin that is left over after one hole has been doped into the ladder. In the t-J chain the spin and charge excitations are carried by different soliton excitations which are far apart in space from each other. This is a typical feature of spin-charge separation and such a system is called a Luttinger liquid. In a Fermi liquid on the other hand they are bound and the excitations are described by quasiparticles carrying both charge and spin.

We have calculated the hole-spin correlations to answer the question if spin-charge separation occurs in the ladder. The real space correlations

$$\langle n_{h,a}(j+r)S^z_{a'}(j)\rangle, \tag{16}$$

are shown in Fig. 11. This correlation function is nonzero for the ground state in the subspace of $S^z_{\rm tot} = \frac{1}{2}$ since there remains one spin unpaired.

The result shows that the hole is tightly bound to the remaining free spin. At strong inter-chain coupling $J' \gg J, t$ it is again predominantly on the same rung. At isotropic coupling the spin-hole bound state is more extended. These spin-hole bound states thus carry both charge and spin. In this sense they are similar to the quasiparticles in a Fermi liquid. This is in contrast to the spin-charge separation in the single chain. We will therefore call the single holes bound to the free spin "quasiparticles", although the system has a spin gap.

V. EXCITATION SPECTRA OF THE LADDER WITH TWO HOLES

A. Excitation Spectra

The ground state of the ladder doped with two holes is, as discussed above, a bound state of the two holes. This bound pair coherently propagates along the ladder, giving rise to the lowest-lying band. When $J' \gg J$, this band, spin-singlet charge excitations, is clearly seen in the numerical results as shown in Fig. 12.

The higher energy excitations are again understood simply in the large J' limit. An essential difference from the lowest-lying singlet band is that two holes are now separate rather than forming a bound pair. Being separate, they can gain a larger kinetic energy, but only in

return for a even larger cost of exchange energy $\sim J'$ as one more singlet rung is broken. Thus there are continua of scattering states of the two holes ("quasiparticles") at higher energies. Since the residual interactions between the two quasiparticles are weak, the energy is almost degenerate between the $S = 0$ and $S = 1$ spin subspaces. On the finite lattice we naturally do not see a continuum of scattering states, but only several discrete bands. These bands, and the fact that the energies of the triplet and singlet are nearly degenerate (up to boundary effects) can be seen in the spectra.

There are various combinations of the two quasiparticle bands in the two quasiparticle continuum of states. The lowest are scattering states of two bonding quasiparticles, with $k_y = 0$. Higher states are scattering states of one bonding and one anti bonding quasiparticle. Having the same transverse momentum, $k_y = \pi$ these states hybridize with the one-magnon excitations in the spin background, resulting in a "bound state" below the two-particle continuum. This is nearly dispersionless and clearly seen in the spectrum. The continua of two antibonding quasiparticles is much higher in energy and not included in the figure.

At higher energies there are spin excitations in the spin background. They are not described by the quasiparticles and will be discussed in more detail in the next section.

The results in the isotropic case, $J'/J = 1$, is shown in Fig. 13. The energy spectrum is more complicated but the above description still holds qualitatively.

The ground state is still the bound hole pair. It moves coherently along the ladder, yielding a gapless band of singlet charge excitations. The band has a linear dispersion around $\mathbf{k} = (0, 0)$ compared with quadratic in the large J' case. An important point is that despite its complicated dispersion the low energy part is well separate from the other excitations. Therefore also at isotropic coupling the only low-energy excitation is the collective charge excitations, and we may identify the isotropic t-J ladder as Luther-Emery liquid. We will discuss the essential role of these charge fluctuations concerning superconductivity in Sec. VI B.

In addition to the gapless band of charge fluctuations, there are various local minima at higher energies. However, they can be explained by taking account of the non-monotonic dispersion of the one-hole spectra shown in Fig. 9, and our quasiparticle picture still holds. More specifically, there are four local minima in the single-hole spectra at $\mathbf{k} \approx (\pm\frac{3}{5}\pi, 0)$ and $\mathbf{k} \approx (\pm\frac{2}{5}\pi, \pi)$, which have nearly the same energy. Thus to construct low-energy two-quasiparticle excitations there are many possible combinations of different minima of one-particle states as discussed below. This is the origin of many local minima in the two-particle spectra and this is confirmed by the fact that the dependence on the boundary condition is consistent with this picture.

The ground state of the two-hole spectrum can be constructed from holes near $\pm k_F$ in the single-hole spectra. The other minima can be explained similarly. The minimum in the PBC spectrum at $k_x = \frac{4}{5}\pi$ can be identified with the $2k_F$ excitation, where a particle moves from one Fermi point to the opposite one. ($2\times\frac{\pm 3}{5}\pi \equiv \frac{\pm 4}{5}\pi$). When using APBC we do not have the k-value of $\pm\frac{3}{5}\pi$ in the single-hole spectrum on an $L = 10$ ladder. The closest k_x-points are $\pm\frac{5}{10}\pi$ and $\pm\frac{7}{10}\pi$, leading to minima at $\pm\pi$ and $\pm\frac{3}{5}\pi$ in the two-hole spectra. Another feature that can be explained from the single hole spectra is the minimum at $\mathbf{k} = (\pi, \pi)$ (odd parity, $k_x = \pi$). Using PBC this state is obtained with one hole with $\mathbf{k} = (\frac{3}{5}\pi, 0)$ and one with $\mathbf{k} = (\frac{2}{5}\pi, \pi)$, leading to the minimum at (π, π).

Using APBC's we can combine one hole at $\mathbf{k} = (\frac{3}{10}\pi, \pi)$ with one at either $\mathbf{k} = (\frac{5}{10}\pi, \pi)$ or $\mathbf{k} = (\frac{7}{10}\pi, \pi)$. As mentioned above these two states are higher in energy than the minimum at $\pm\frac{3}{5}\pi$ and very similar in energy. Therefore we expect two states at $\mathbf{k} = (\frac{4}{5}\pi, \pi)$ and $\mathbf{k} = (\pi, \pi)$ which are similar in energy but at a higher energy than the corresponding states with PBC. This is exactly what we observe. The odd parity states near $k_x = 0$ can be constructed similarly.

The qualitative features of the three-hole excitation spectrum can again be explained similarly.

B. Spin Excitations

One of the most interesting properties of the t-J ladder is that there are two distinct types of spin excitation. Although it is most easily seen in the large J' limit, the qualitative distinction remains down to the isotropic point.

The first type is the collective magnon excitations inherited from the undoped spin ladder. One of the electron-filled rungs is now excited to a spin triplet. This local excitation is what we call "magnon" and it propagates coherently along the ladder, leading to an energy dispersion with respect to k_x. For a detailed investigation, we have examined the two-hole spectra in more detail and have calculated the spin-spin and spin-hole correlations of the low-lying triplet states. We find that the magnon excitations of the Heisenberg ladder evolve continuously upon doping. However there discontinuously appears a new kind of spin-triplet excitation at lower energies, which is not present in the undoped ladder.

The lowest excitation is a different type for which quasiparticles play an essential role. Therefore, the spin gap, defined as the excitation energy to the lowest triplet, is a discontinuous function of the hole doping at $\delta = 0$. This new type of excitations consists of breaking a pair of holes into two separate quasiparticles, each carrying charge $+|e|$ and spin $1/2$.[28] When the two quasiparticles are both in the bonding orbital, their lowest energy, at $\mathbf{k} = (0, 0)$, is lower than the lowest magnon excitation. The additional energy gain is easily understood, since the two separate holes have a larger kinetic energy of the order of t while the gain of the magnon kinetic energy is the order of t^2/J'. As was shown in Fig. 5, down to the

isotropic point the lowest two-quasiparticle excitation is lower in energy than the lowest magnon excitation.

The above picture is confirmed by comparing the correlation function between the two different states. The dynamical spin structure factor gives another confirmation.

Figure 14 shows the equal-time correlations of the two holes, $\langle n_{\rm h}(\mathbf{r})n_{\rm h}(\mathbf{0})\rangle$, and of spin and hole, $\langle S^z(\mathbf{r})n_{\rm h}(\mathbf{0})\rangle$, calculated for these two types of spin-triplet excitations. The latter quantity is nonzero since the states with $S^z = 1$ are used in the calculation. When $J'/J = 10$, the two holes are separate in space in the lowest state, while tightly bound in the other state. The position of magnetic excitation is, on the other hand, close to the hole position in the lowest state, while they are far apart from each other in the other state. These two behaviors are what is predicted by our picture explained above, and despite modification in small detail they are qualitatively consistent even at the isotropic point.

Our numerical results confirm that the lowest triplet state is the quasiparticle excitation where the bound hole pair breaks up. The two holes repel each other and the hole-hole correlations have the maximum at the largest distance $L/2$. Each of the holes is bound to a spin-1/2, as can be seen from the hole-spin correlation function. This state is sketched in Fig. 4(d).

As a typical magnon excitation, we show the correlations for the state at $\mathbf{k} = (\pi, \pi)$ that has the main spectral weight in the dynamical spin structure factor which will be discussed soon. The hole-hole correlations are similar to the ground state. The hole-spin correlations show that the triplet carrying spin current is far away from the hole pair. This state is shown in Fig. 4(e). Mean field theory[5] predicts only this magnon excitation, which evolves continuously from the Heisenberg ladder.

In neutron scattering experiments the relevant quantity is the dynamical spin structure factor

$$\mathcal{S}(\mathbf{q},\omega_0) \equiv \sum_n \left|\langle n|S^z_{\mathbf{k}}|\text{G.S.}\rangle\right|^2 \delta(E_n - E_{\text{G.S.}} - \omega_0), \quad (17)$$

where $|n\rangle$ is the complete set of eigenstates with energy E_n, $|\text{G.S.}\rangle$ is the ground state with energy $E_{\text{G.S.}}$ and

$$S^z_{\mathbf{q}} \equiv \frac{1}{\sqrt{2L}} \sum_{\mathbf{r}} e^{i\mathbf{q}\cdot\mathbf{r}} S^z_{\mathbf{r}}. \quad (18)$$

Figure 15 shows $\mathcal{S}(\mathbf{q},\omega)$ calculated for the Heisenberg ladder using the Lanczos diagonalization combined with the continued fraction method.[29] It can clearly be seen that the dominant contributions arise from the collective excitations near $\mathbf{q} = (\pi, \pi)$ and there is very little weight in the continuum of spin excitations at higher energy.

In the doped case the two types of spin excitations have different contributions to the dynamical spin structure factor. It can be seen in Fig. 16 that the continuum of spin excitations move towards lower energies. Most of the weight is in the magnon excitations, consistent with the mean-field theory,[5] and there is very little weight in the lowest triplet excitation consisting of the two separate quasiparticles.

As in the large J' limit the lowest triplet excitation with $q_y = \pi$ is a bound state of a spin triplet and the hole pair. At $\mathbf{q} = (\pi, \pi)$ this state has no spectral weight, while most of the weight is in the second excited state, which has the triplet separated from the bound pair. This is a finite size effect of the two-hole system. The reason is that at $q_y = 0$ or π we have an additional symmetry, reflection invariance in the ladder direction. The parity under these reflections is different for the ground state and the triplet-hole pair ground state, leading to the vanishing weight.

A significant difference between the two types of spin excitations is that the largest number of "quasiparticle" excitations is limited by the number of holes. We need at least two holes to create such an excitation. The number of possible excitations is thus proportional to the hole doping δ. On the other hand, the magnon excitations can be excited at any rung where there are no holes. The number of these excitations is thus proportional to $1-\delta$ instead, much larger for a small doping δ. Therefore with decreasing temperature the susceptibility will show a large exponential drop at temperatures of the order of the gap of the undoped system ($T \sim 0.5J$), followed by a small drop at temperatures around the spin gap of the doped system.

To summarize we can describe the spin excitations of the t-J ladders by a simple picture: quasiparticles moving in a spin liquid background. In the ground state the quasiparticles are paired. In the excitation spectrum two types of excitations can be distinguished. The first corresponds to the breaking of a pair of quasiparticles. This excitation has the lowest energy, but its number is limited by the number of holes. Of more importance for measurements of the susceptibility or inelastic neutron scattering experiments is the second type, which are magnon excitations in the spin liquid background. They evolve continuously from the undoped Heisenberg ladder. Although the gap for this type of excitation is larger it is more important since we can excite more of these excitations. Also the weight in the dynamical spin structure factor is larger.

C. Charge Excitations

Similarly to the calculation of the dynamical spin structure factor we calculate the dynamical charge structure factor defined by

$$\mathcal{N}(\mathbf{q},\omega_0) \equiv \sum_n \left|\langle n|\rho_{\mathbf{q}}|\text{G.S.}\rangle\right|^2 \delta(E_n - E_{\text{G.S.}} - \omega_0), \quad (19)$$

where $\rho_{\mathbf{q}}$ is the Fourier transform of the local density fluctuation around the average density ρ.

The result of our calculations is shown in Fig. 17. The main contribution arises from the coherent motion of the hole pairs. This leads to large peaks at low energies near $\mathbf{q} = (0, 0)$. The rest of the weight is distributed incoherently over a wide region at rather high energies of order $4t$. It arises from interactions of a single hole with the surrounding spin background. This is similar to results obtained for two dimensions.[30]

Recently Tohyama et al. have calculated $\mathcal{S}(\mathbf{q}, \omega)$ and $\mathcal{N}(\mathbf{q}, \omega)$ for single chains and 2D clusters.[31] In the single chain they find that, as expected from Luttinger liquid theory, the charge and spin excitations are decoupled in the low energy region. The dynamical charge structure factor is very similar to that of spinless fermions, consisting of large peaks at the energies expected from the cosine band of the spinless fermions.

In two dimensions they find different behavior. In the spin structure factor nearly all of the weight is in a few sharp peaks at low energies. In the charge structure on the other hand the main weight is at relatively large energies, of the order of several t, and it strongly broadened. This is indicative of strong spin-charge interactions. Only at some special $\mathbf{q}$-points are there peaks at low energies. The dynamical charge structure factor, $\mathcal{N}(\mathbf{q}, \omega)$ for the ladder shown in Fig. 17 differs a lot from the single chain but resembles the 2D cluster. At large q_x, we see the peaks at large energies $\sim 2t$-$4t$. At small q_x in the $q_y = 0$ sector, $\mathcal{N}(\mathbf{q}, \omega)$ for the ladder is dominated by the collective mode of the hole pairs, and its behavior differs substantially from spinless fermions. Another similarity to the 2D system is found in the dynamical spin structure $\mathcal{S}(\mathbf{q}, \omega)$ where the main weight is in peaks with energies $\sim J$ (see Fig. 16). We conclude from this comparison that the 2D clusters and the ladders are closely related - a fact which points towards a "d-wave" paired state for the 2D clusters. A more difficult question is to what extent this behavior of the finite 2D cluster is a consequence of the strong tendency of finite clusters to favor singlet ground states and to what extent it is representative of an infinite plane.

VI. LONG RANGE CORRELATIONS

A. Superconducting Correlations

A highly intriguing and much debated subject of the high-T_c superconductors is the internal symmetry of the order parameter. In this section we study the internal structure of the pairs in the doped ladders. For the t-J model usually only nearest-neighbor pairs have been considered except for a few cases. It is reasonable to assume that they are the dominant pair correlations. However more quantitatively we have chosen the optimal form for the pairs.

Using the Lanczos algorithm we calculate the pairing correlation functions for different pairings. Let us introduce the operator creating a singlet pair of electrons on sites $\mathbf{r}$ and $\mathbf{r} + \mathbf{d}$,

$$P^\dagger_{\mathbf{r},\mathbf{d}} = \frac{1}{\sqrt{2}} \left(c^\dagger_{\mathbf{r},\uparrow} c^\dagger_{\mathbf{r}+\mathbf{d},\downarrow} - c^\dagger_{\mathbf{r},\downarrow} c^\dagger_{\mathbf{r}+\mathbf{d},\uparrow} \right), \tag{20}$$

Using this definition of the pair operator we can calculate the superconducting order parameter

$$\chi_{\mathbf{d}} = \Big\langle \text{G.S., } N_\text{h}\text{−2 holes} \Big| \frac{1}{2L} \sum_{\mathbf{r}} P^\dagger_{\mathbf{r},\mathbf{d}} \Big| \text{G.S., } N_\text{h} \text{ holes} \Big\rangle \tag{21}$$

and its Fourier transform

$$\begin{aligned} \chi_{\mathbf{k}} &= \sum_{\mathbf{k}} \chi_{\mathbf{d}}\, e^{i\mathbf{k}\cdot\mathbf{d}} \\ &= \big\langle \text{G.S., } N_\text{h}\text{−2 holes} \big| P^\dagger_{\mathbf{k},-\mathbf{k}} \big| \text{G.S., } N_\text{h} \text{ holes} \big\rangle \end{aligned} \tag{22}$$

where $P_{\mathbf{k},-\mathbf{k}}$ is the Fourier transform of the real space pair operator with zero total momentum.

Figure 18 shows the superconducting order parameter for the $L = 8$ ladder with PBC's for several values of J/t. The most obvious properties are that the sign is opposite for pairs with $k_y = 0$ and $k_y = \pi$ and that the absolute values are very small near $(0, 0)$ and (π, π). This is similar to d-wave pairing in a fully 2D system. The absolute value is largest near wave vectors which we have identified with the Fermi points of the quasiparticles $\mathbf{k} = (3\pi/4, 0) \approx \mathbf{k}^B_F$ and $\mathbf{k} = (\pi/2, \pi) \approx \mathbf{k}^A_F$. At large J/t the order parameter is very similar to the simple $\cos k_x - \cos k_y$ structure of nearest neighbor d-wave pairs.

Consider now pairs with a form factor F:

$$P^\dagger_{\mathbf{r}} = \sum_{\mathbf{d}} F^*_{\mathbf{d}}\, P^\dagger_{\mathbf{r},\mathbf{d}}, \tag{23}$$

where F is normalized

$$\sum_{\mathbf{d}} |F_{\mathbf{d}}|^2 \equiv 1. \tag{24}$$

A simple calculation shows that the superconducting "order parameter"

$$\chi_F = \sum_{\mathbf{d}} F^*_{\mathbf{d}}\, \chi_{\mathbf{d}} \tag{25}$$

is maximized by the pair with the form factor

$$F_{\mathbf{d}} = \frac{\chi_{\mathbf{d}}}{\left[\sum_{\mathbf{r}} |\chi_{\mathbf{r}}|^2 \right]^{1/2}}, \tag{26}$$

which is proportional to the order parameter $\chi_{\mathbf{d}}$. This optimal order parameter then is

$$\chi = \left[\sum_{\mathbf{d}} |\chi_{\mathbf{d}}|^2 \right]^{1/2}. \tag{27}$$

In Fig. 19 we show this maximal order parameter for a $L = 8$ ladder as a function of J/t. A clear increase as a function of J/t can be seen, similar to single chains and 2D planes where the superconducting correlations are also enhanced at larger J values. We note that the expectation value of the optimal order parameter is larger for four doped holes than for two holes. This is a consequence of the strong correlation effect, as any pairing order parameter or fluctuations should vanish as $\delta \to 0$. The mean-field theory including the strong correlation effects predicts a δ-linear dependence of the order parameter as $\delta \to 0$:[5] i.e., the superfluid density is proportional to the hole doping. Our results show that the value for four doped holes is less than twice the value for two holes. This may be because that in the four hole case the doping, $\delta = 0.25$, is already large and out of the region of δ-linear dependence. We need further study using larger lattices to clarify this point more quantitatively.

B. Mapping to a Luther-Emery Liquid

In Secs. III-V, our numerical results have shown that all the spin excitations cost a finite energy and the only gapless excitations are charge fluctuations, i.e., coherent propagation of bound hole pairs along the ladder direction. We may therefore say that the system is a Luther-Emery liquid[25] from large J' limit down to the isotropic coupling. This observation indicates that the low-energy and long-wavelength properties of lightly doped t-J ladders would be entirely described by an effective continuum Hamiltonian in terms of charge degrees of freedom and this model correctly predicts long-range asymptotic behavior of correlation functions. The effective model is actually the bosonic Gaussian model proposed by Efetov and Larkin,[32]

$$\mathcal{H}_{\rm EL}= \frac{\pi}{2}\int dx \left\{ \frac{[n_B(x)-\overline{n}_B]^2}{\pi K_{\rm B}} + \pi K_{\rm B} v_s^2 \Big[\frac{\nabla\theta_B(x)}{\pi}\Big]^2 \right\}, \quad (28)$$

where $n_B(x)$ represents the density of bound hole pairs at the rung x with the average value $\overline{n}_B \equiv N_B/L = \delta$, and $\theta_B(x)$ is its conjugate phase obeying the canonical commutation relation, $[n_B(x), \theta_B(x')] = i\delta(x-x')$. As shown by the fact that the $q = 0$ mode of the first term in Eq. (28) denotes the change in the ground state energy associated with the number of bound hole pairs, $\Delta E \propto (1/2K_B)(\Delta N_B)^2$, the parameter $K_{\rm B}$ is given by the compressibility of the hole pairs, which will be shown afterwards. The second term, on the other hand, describes the energy change associated with current, related with the sound velocity v_s. Instead of a direct calculation of the dispersion relation, the sound velocity can also be obtained numerically by applying an Aharanov-Bohm flux penetrating in the center of the ladder with PBC's, since the flux induces a finite current along the chain direction. Once the two parameters, v_s and $K_{\rm B}$, are determined in this way, it is straightforward to calculate the power-law exponents of correlation functions as follows.

The Efetov-Larkin Hamiltonian is actually identical to the single-component (i.e., spinless) Luttinger model diagonalized by bosonization, which was studied by Mattis and Lieb,[33] Luther and Peschel,[34] and Haldane[26] in details. The Hamiltonian (28) is immediately solved by rewriting each Fourier component with a boson operator,

$$n_{B,k} \equiv \sqrt{\frac{|k|}{2\pi}}\big(b_k + b_{-k}^\dagger\big), \quad \theta_{B,k} \equiv i\sqrt{\frac{\pi}{2|k|}}\big(b_k^\dagger - b_{-k}\big), \quad (29)$$

then the result is

$$\mathcal{H}_{\rm EL} = \sum_{|k|} v_s|k| b_k^\dagger b_k + \frac{\pi}{2L}\Big[v_N(N_{\rm B}-N_{\rm B}^0)^2 + v_J J_{\rm B}^2\Big]. \quad (30)$$

Here N_B is the total number of bound hole pairs and $v_N = (\pi K_{\rm B})^{-1}$ is the charge velocity and $v_J = \pi K_{\rm B} v_s^2$ is the current velocity associated with the number of $2k_F^{\rm SF}$ excitations, $J_{\rm B}$, obeying the universal relation, $v_N v_J = v_s^2$. Here $k_F^{\rm SF} = \pi\delta = \pi(1-\rho)$ is the Fermi wave number of spinless fermions transmuted from the bosonic hole pair operators by the Jordan-Wigner transformation. The last two terms in Eq. (30) describe non-bosonic excitations accompanied with the change in the quantum numbers, $N_{\rm B}$ and $J_{\rm B}$. Their importance was first pointed out by Haldane in his Luttinger liquid concept.[26]

The propagator of bound hole pair, i.e. pairing correlation, is then obtained as in the calculation of the Debye-Waller factor,

$$\begin{aligned} G(r) &= \overline{n}_B \left\langle e^{i[\theta_B(r)-\theta_B(0)]}\right\rangle = \overline{n}_B\, e^{-\langle[\theta_B(r)-\theta_B(0)]^2\rangle/2} \\ &\propto r^{-1/K_\rho}, \end{aligned} \quad (31)$$

where the exponent is

$$K_\rho = 2\pi K_{\rm B} v_s = \pi\rho^2\, v_s\, \kappa, \quad (32)$$

where ρ is the electron density per site and κ is the electron compressibility. The relation for the ladder, $K_B = \kappa\rho^2/2$, is used to obtain the second equality. This result differs from the one for the chain, which has the numerical factor $\pi/2$ instead. It is important to emphasize that this result is the Luttinger liquid parameter, $K_\rho = 2(v_J/v_N)^{1/2}$, for the single-component boson systems.

Density-density correlations are characterized by a power-law decay at the wave number $2k_F^{\rm SF}$. Since $k_F^{\rm SF}$ is twice the average of the Fermi wave number of the original electron bonding and antibonding bands, $k_F = \frac{\pi}{2}\rho$, the wave number $2k_F^{\rm SF}$ is actually $4k_F$ in the original picture. The exponent of the $2k_F^{\rm SF}$=$4k_F$ CDW fluctuations is calculated using a density-phase duality as was done in the original paper.[32] The density operator has a short-range $2k_F^{\rm SF}$ CDW order, but since the value of $2k_F^{\rm SF}$ is locally determined by the density at each position, it is

fluctuating around the average value $2\pi\delta$ associated with the density fluctuations. We therefore may write as

$$n_B(x) = \overline{n}_B \cos\bigl[2k_F^{\rm SF}x + 2\theta_J(x)\bigr], \tag{33a}$$

$$\frac{\partial\theta_J}{\partial x} = \pi(n_B - \overline{n}_B). \tag{33b}$$

Rewriting the Hamiltonian (28) with θ_J and its conjugate operator $n_J \equiv \frac{1}{\pi}\nabla\theta_B$, we again obtain a Gaussian model,

$$\mathcal{H}_{\rm EL} = \frac{\pi}{2}\int dx \left\{ v_J\bigl[n_J(x)\bigr]^2 + v_N\Bigl[\frac{\nabla\theta_J(x)}{\pi}\Bigr]^2\right\}, \tag{34}$$

where $[n_J(x), \theta_J(x')] = i\delta(x-x')$. This duality of the charge and current operators was also emphasized in the Haldane's paper.[26] Since the density-density correlation is written as an exponential of θ_J in this representation, its calculation can be done similarly as before,

$$\begin{aligned} N_B(r) &\equiv \langle n_B(r) n_B(0)\rangle \approx {\overline{n}_B}^2 \cos(2k_F^{\rm SF} r)\langle e^{2i[\theta_J(r)-\theta_J(0)]}\rangle \\ &\propto \cos(2k_F^{\rm SF} r)\, r^{-K_\rho}. \end{aligned} \tag{35}$$

Instead of calculating the sound velocity, the value of K_ρ is more accurately obtained through the Drude weight defined by

$$D \equiv \frac{L}{2}\left.\frac{\partial^2 E_{\rm G.S.}(\phi)}{\partial\phi^2}\right|_{\phi=0}, \tag{36}$$

where $E_{\rm G.S.}(\phi)$ is the total energy of the ground state when the flux ϕ is penetrating. Assuming the holes propagate in pair, the relation between D and v_s for the ladder is obtained and the result agrees with the one for the chain[35] aside from its numerical factor,

$$D = \frac{4}{\pi}\, v_J = \frac{2}{\pi}\, K_\rho v_s\ . \tag{37}$$

Combined this with Eq. (32), we finally obtain the formula of the correlation exponent in terms of the compressibility and the Drude weight:

$$K_\rho = \pi\,\rho\,\sqrt{\frac{\kappa D}{2}}. \tag{38}$$

It is noted that this expression is identical to the one for the chain in terms of κ and D, while they differ by factor 2 in terms of κ and v_s.

In this way, when the energy scale concerned is smaller than the spin gap, we can predict long range asymptotic behavior of the correlation functions based on the Efetov-Larkin effective model, and calculate correlation exponents once the two parameters, v_s and $K_{\rm B}$ (or equivalently κ and D), are numerically determined.

Figure 20 shows the correlation exponent calculated in this way for the isotropic ladder ($J'/J = 1$) with $L = 7$ and two holes as a function of J. This corresponds to the electron density, $\rho = \frac{6}{7} = 0.857$. The necessary quantities are carefully calculated by using the Lanczos diagonalization. The compressibility, κ, is determined from the ground state energy of unfrustrated systems in the sense explained before. The Drude weight, D, is then calculated by Eq. (36). Combining these two, K_ρ is obtained via Eq. (38).

Near the phase separation boundary, K_ρ grows rapidly. This is owing to the divergence of the compressibility at this boundary. In other words, the collective charge excitations become softening and the superconducting fluctuations are enhanced correspondingly.

Recently Hayward et al.[36] directly calculated various correlation functions for the t-J ladders by using the density-matrix renormalization-group method. At $J/t = J'/t = 1$ and $\rho = 0.8$, they found a power-law decay of the pairing correlations with the exponent close to unity. This exponent corresponds to $K_\rho \sim 1$, which is larger than our estimate at the same J and J', $K_\rho \approx 0.7$.[7] The discrepancy may be owing to the larger electron density in our calculation, $\rho = \frac{6}{7} = 0.857$, but it is not clear if this suffices to account for the difference until new calculation is carried out at the same density. Hayward et al. also report data on the density-density correlation function[36] but the exponent of the expected power-law decay of the oscillatory term cannot be easily extracted.

VII. ONE-PARTICLE EXCITATIONS

Finally we discuss the one-particle Green's function where we can see the quasiparticle excitations directly. The electron and hole parts of its spectral function are defined as

$$\begin{aligned} A_{{\rm e},\sigma}(\mathbf{k},\omega) &\equiv \sum_n \Bigl|\langle n, 2L{-}1|c^\dagger_{\mathbf{k}\sigma}|{\rm G.S.}, 2L{-}2\rangle\Bigr|^2 \\ &\quad\times\delta(\omega - E_n(2L{-}1) + E_{\rm G.S.}(2L{-}2) + \mu), \\ A_{{\rm h},\sigma}(\mathbf{k},\omega) &\equiv \sum_n \Bigl|\langle n, 2L{-}3|c_{\mathbf{k}\sigma}|{\rm G.S.}, 2L{-}2\rangle\Bigr|^2 \\ &\quad\times\delta(\omega + E_n(2L{-}3) - E_{\rm G.S.}(2L{-}2) + \mu), \end{aligned} \tag{39}$$

where $|n, N\rangle$ is an eigenstate for N electrons with the energy $E_n(N)$ and $|{\rm G.S.}, N\rangle$ denotes the ground state with N electrons. Positive (negative) energies correspond to the electron (hole) part. The chemical potential is defined by

$$\mu \equiv \tfrac{1}{2}\bigl[E_{\rm G.S.}(2L{-}1) - E_{\rm G.S.}(2L{-}3)\bigr]. \tag{40}$$

The results for $L = 10$ and the isotropic couplings, $J'/J = 1$, are shown in Figs. 21 for J/t=0.3 and 0.5. The wave vectors along the ladder $k_x = \frac{2\pi}{L}n$ (n: integer) are for PBC's and $k_x = \frac{2\pi}{L}(n+\frac{1}{2})$ for APBC's. The ground state energy $E_{\rm GS}(2L-2)$ and the chemical potential μ in Eq. (39) are the average over both boundary conditions. The results for $L = 10$ are very similar to our $L = 8$ results published before.[3]

The spectral function has large weights for the bonding (B) ($k_y = 0$) and antibonding (A) ($k_y = \pi$) orbitals only near the Fermi energy $\omega = 0$, and they seem to constitute quasiparticle bands. Away from the Fermi energy, the individual quasiparticle peaks are much less prominent and there is an incoherent part with an energy of the order of t.

The quasiparticle part of the spectrum is consistent with the mean-field theory based on the d-wave RVB state.[5] The undoped ladder consists of local singlets on the rungs. Such a singlet is the superposition of two electrons in the bonding orbital and two electrons in the antibonding orbital, $b^\dagger_\uparrow b^\dagger_\downarrow - a^\dagger_\uparrow a^\dagger_\downarrow |0\rangle$. Holes doped into the half-filled ladder will go predominantly into the antibonding orbitals to gain a larger kinetic energy along the rung direction. The bonding band is occupied by more electrons, while the antibonding band is occupied by less electrons. The quasiparticle with energy closest to $\omega = 0$ has a wave vector nearest to the original Fermi wave number, k_F: ($k_x = \frac{3\pi}{5}$ for bonding and $k_x = \frac{2\pi}{5}$ for antibonding). Because of the band splitting, $k_F^{\rm B} > k_F^{\rm A}$, but the Luttinger sum rule is satisfied, $k_F^{\rm B} + k_F^{\rm A} = (1-\delta)\pi$. This means the Fermi volume is large, proportional to the electron number rather than the hole number, and this is consistent with photo-emission experiments on cuprate superconductors.[37] It is important to notice that the quasiparticle peaks near the Fermi energy have their counterparts on the opposite side of the Fermi energy. An electronic quasiparticle peak at energy $\omega > 0$ has a shadow hole peak at energy around $-\omega < 0$, and *vice versa*. These peaks indicate that the quasiparticle excitations are those of the Bogoliubov quasiparticles as in BCS theory, *i.e.*, mixture of an electron and a hole ($\alpha^\dagger_{\mathbf{k}} = u_{\mathbf{k}} c^\dagger_{\mathbf{k}\uparrow} + v_{\mathbf{k}} c_{-\mathbf{k}\downarrow}$). The weights in the electron and hole parts are proportional to $|u_{\mathbf{k}}|^2$ and $|v_{\mathbf{k}}|^2$. They are hole-like around $k_x = 0$ and electron-like around $k_x = \pi$ for both the bonding and antibonding bands.

There exists a finite energy gap in the quasiparticle spectra. The electron and hole branches both come close to the Fermi energy at $k_x \sim \frac{\pi}{2}$, but instead of passing through they move away from it. The energy gap for $J/t = 0.3$ (0.5) is $0.13t$ ($0.29t$) at $\mathbf{k} = (\frac{3\pi}{5}, 0)$ and $0.22t$ ($0.39t$) at $\mathbf{k} = (\frac{2\pi}{5}, \pi)$. This corresponds to a quasiparticle gap $2\Delta_{\rm QP} \simeq 0.13t \simeq \frac{J}{2}$ for $J/t = 0.3$ and $2\Delta_{\rm QP} \simeq 0.29t \simeq \frac{3J}{5}$ for $J/t = 0.5$.

It is interesting to note that the calculations of $A(\mathbf{k}, \omega)$ in 2D clusters[38,39] show similar behavior for $\mathbf{k}$-points not along $(1,1)$ but no shadow peaks for $\mathbf{k} \parallel (1,1)$, indicating $d_{x^2-y^2}$-pairing also.

Figure 22 shows the spectral function of the one-particle Green's function of two holes in an $L = 10$ ladder summed over all wave vectors: $A_{{\rm e},\sigma}(\omega) = \sum_{\mathbf{k}} A_{{\rm e},\sigma}(\mathbf{k}, \omega)$, and $A_{{\rm h},\sigma}(\omega) = \sum_{\mathbf{k}} A_{{\rm h},\sigma}(\mathbf{k}, \omega)$. This quantity is the local density of states to add and remove electrons. In a strongly correlated system, the sum rules on the weight (i.e., the integrated values) of $A_{\rm e}(\omega)$ and $A_{\rm h}(\omega)$ are very different since the former is given by the number of empty sites and the latter by the number of filled sites (or equivalently the number of holes and electrons, respectively). In a Fermi liquid the values of $A_{\rm e}(\omega)$ and $A_{\rm h}(\omega)$ for small values of $|\omega - \mu|$ are determined by quasiparticle weight at the Fermi energy and are continuous. It is interesting therefore to note that Fig. 22 shows approximately similar values for $A_{\rm e}(\omega - \mu)$ and $A_{\rm h}(\mu - \omega)$ around $\omega \sim \mu$, but the sum rule on the total weight is satisfied through the large weight in incoherent excitations in $A_{\rm h}(\omega)$ at higher energies, $|\omega - \mu| > J$. The strong correlation condition is reflected in the much smaller total weight in $A_{\rm e}(\omega)$ which comes about through an effective cut-off in energy on $A_{\rm e}(\omega)$. In this respect the system in energy space is similar to a lightly hole doped band insulator although as we discussed earlier the location in $\mathbf{k}$-space of the coherent quasiparticle peaks corresponds to a large Fermi surface to add and remove electrons.

The momentum distribution for electrons, $n^{\rm e}_\sigma(\mathbf{k}) \equiv \langle c^\dagger_{\mathbf{k},\sigma} c_{\mathbf{k},\sigma} \rangle$, and for holes, $n^{\rm h}_\sigma(\mathbf{k}) \equiv \langle c_{\mathbf{k},\sigma} c^\dagger_{\mathbf{k},\sigma} \rangle$, is shown in Fig. 23. Note because of the strong correlation condition, these do not add to one but instead their sum is given by $n^{\rm e}_\sigma(\mathbf{k}) + n^{\rm h}_\sigma(\mathbf{k}) = \frac{1}{2}(1 + \delta)$. The strong correlation condition is also evident in the reduced magnitude of the variation of $n^{\rm e}_\sigma(\mathbf{k})$ as a function of $\mathbf{k}$. Nonetheless the presence of an apparent "Fermi surface" in the center of the Brillouin zone is clear, consistent with the dispersion relations of the coherent quasiparticles. The difference between the bonding ($k_y = 0$) and antibonding ($k_y = \pi$) bands and the reduced occupation of the antibonding band arise from the energy gain in placing the doped holes preferentially in the antibonding band.

VIII. CONCLUSIONS

The results of our Lanczos diagonalizations confirm earlier studies which concluded that lightly doped two-leg ladders belong to a different universality class from single chains. The latter are Tomonaga-Luttinger liquids with gapless and separated spin and charge excitations. The ladder in contrast has a finite gap in the spin excitation spectrum and gapless excitations only in the charge sector. The low energy excitations evolve continuously from the limit of strong inter-chain exchange coupling ($J' \gg J, t$) and the simplicity of that limit allows a clear interpretation of our results.

At large J' the dispersion relation of a single doped hole consists of two cosine bands corresponding to bonding and antibonding states on a rung. Lowering J' to the isotropic limit ($J'/J = 1$) and setting both $J, J' < t$ changes the dispersion relation substantially. The coherent parts of both bands are centered at energies $\sim -1.5t$ but the width is $\sim J$ only. The spin and charge components are still bound but more loosely and the large magnetic polarizability of the spin background introduces longer-range hoppings. Remarkably the form of

the bands resembles the noninteracting band structure so that a photoemission experiment which removes electrons would measure in effect a large "Fermi surface" with bonding and antibonding pieces. In this regime the quasiparticle propagation is strongly influenced by the coupling to magnetic excitations.

When two holes are added they bind together on a single rung at large J' and remain bound although the size of the bound hole pair increases as J' approaches $J \sim t/2$. Moreover the qualitative features of the density-density $\mathcal{N}(\mathbf{q},\omega)$ and spin-spin structure factor $\mathcal{S}(\mathbf{q},\omega)$, which are easy to understand at large J', remain similar as J' approaches $J \sim t/2$. $\mathcal{N}(\mathbf{q},\omega)$ near $\mathbf{q} = (0,0)$ is dominated by the low energy mode associated with the motion of hole pairs. At large q_x, $\mathcal{N}(\mathbf{q},\omega)$ has a broad peak at high energies ($\sim 4t$) similar to that found by Ohta, Eder and Maekawa for 2D clusters.[39] They interpreted this as local excitations of single holes in the magnetic cloud or spin bag.[30] The dynamical spin structure factor, $\mathcal{S}(\mathbf{q},\omega)$, also resembles 2D clusters and not 1D chains when we compare to the results of Tohyama, Horsch and Maekawa.[31] The major weight is at energies $\sim J$. The spin gap evolves discontinuously upon doping through the new quasiparticle excitations that can be made by breaking a hole pair into two separate single holes. However the major weight of the spin excitations remains in the collective magnon mode whose dispersion evolves continuously from the $\delta = 0$ limit, although it is influenced by the continuum of quasiparticle excitations.

We have also investigated the one-particle spectral functions to add and remove electrons from the two-hole ground state. These show clearly the unusual nature of this "Fermi liquid". When electrons are removed (or holes added), the spectral weight is spread over a large energy region ($\sim 6t$), but the coherent part is limited only to energies $\sim J$ below the Fermi energy μ. The energy dispersion relations show a large apparent Fermi surface for the coherent quasiparticles and which matches onto a similar one for adding electrons at energies greater than μ. These $\mathbf{k}$-space features resemble a metal with a large Fermi surface. The property that resembles a lightly hole doped insulator is the energy dependence of the spectral weight to add an electron. This shows a low energy cutoff ($\sim \delta \cdot 6t$) similar to a lightly hole doped band insulator. The result is an intriguing duality between metallic-like features in $\mathbf{k}$-space and lightly hole doped insulating features in energy space.

The overall properties of the lightly doped ladder place it in the Luther-Emery class rather than the Tomonaga-Luttinger class of 1D systems. The low energy properties of Luther-Emery liquids are described by interacting hard-core bosons as shown by Efetov and Larkin. In the present case the Efetov-Larkin bosons are bound hole pairs. Two features distinguish the t-J ladder from the usual Luther-Emery liquids arising from attractive interactions. One is the d-wave character of the pairing and the second is the presence of magnon excitations and limited quasiparticle excitations. Note the magnon excitations cannot be viewed as the collective mode of quasiparticles since the latter vanish as $\delta \to 0$. The system is not a standard Fermi liquid, but rather is a new and interesting mixture of a dilute attractive Fermi gas in which the hole binding energy remains finite as $\delta \to 0$, and a dense Fermi liquid with an apparent large Fermi surface in $\mathbf{k}$-space.

Comparing the ladder with the results by Tohyama et al., we see that the ladder is very different from the single chain but similar to 2D clusters in many respects. Both in ladders and in 2D clusters d-wave pairs are found down to small J/t. The dynamical charge and spin structure factors look remarkably similar and the single-particle spectral functions indicate the existence of Bogoliubov quasiparticles with a finite superconducting gap. Thus we are lead to the conjecture that the t-J model on 2D clusters is a doped RVB spin liquid showing d-wave pairing, similar to the ladder.

ACKNOWLEDGMENTS

We wish to thank M. Sigrist, F.C. Zhang, H. Monien, R. Noack, D. Poilblanc, P. Prelovsek, D.J. Scalapino, S.R. White, and D. Würtz for helpful discussions. This work has been supported by the Swiss National Fund under grant number NFP-304030-032833, by an internal grant of ETHZ and by the Centro Svizzero di Calcolo Scientifico CSCS Manno. The calculations have been performed on the Cray Y-MP/464 of ETH Zürich and on the NEC SX-3/24R of CSCS Manno.

---

* Current address: Institute for Solid State Physics, University of Tokyo, Roppongi 7-22-1, Tokyo 106, Japan

[1] E. Dagotto, J. Riera, and D. J. Scalapino, Phys. Rev. B **45**, 5744 (1992).
[2] R.M. Noack, S.R. White and D.J. Scalapino, Phys. Rev. Lett. **73**, 882 (1994).
[3] H. Tsunetsugu, M. Troyer and T.M. Rice, Phys. Rev. B **49**, 16078 (1994).
[4] T. M. Rice, S. Gopalan, and M. Sigrist, Europhys. Lett. **23**, 445 (1993).
[5] M. Sigrist, T. M. Rice, and F. C. Zhang, Phys. Rev. B **49**, 12058 (1994).
[6] D. V. Khveshchenko and T. M. Rice, Phys. Rev. B **50**, 252 (1994); D. V. Khveshchenko, *ibid.* **50**, 380 (1994); N. Nagaosa and M. Oshikawa, preprint cond-mat/9412003; H. J. Schulz, preprint cond-mat/9412098.
[7] H. Tsunetsugu, M. Troyer and T.M. Rice, Phys. Rev. B **51**, 16456 (1995).
[8] R. Hirsch, Diplomarbeit Universität Köln, 1988.
[9] S. P. Strong and A. J. Millis, Phys. Rev. Lett. **69**, 2419 (1992).

[10] S. Gopalan, T.M. Rice and M. Sigrist, Phys. Rev. B **49**, 8901 (1994).
[11] T. Barnes, E. Dagotto, J. Riera and E.S. Swanson, Phys. Rev. B **47**, 3196 (1993).
[12] T. Barnes and J. Riera, Phys. Rev. B **50**, 6817 (1994).
[13] S.R. White and R.M. Noack and D.J. Scalapino, Phys. Rev. Lett. **73**, 886 (1994).
[14] M. Troyer, H. Tsunetsugu and D. Würtz, Phys. Rev. B, **50**, 13515 (1994).
[15] M. Takano et al., JJAP Series **7**, 3 (1992); M. Azuma, Z. Hiroi, M. Takano, K. Ishida, Y. Kitaoka, Phys. Rev. Lett. **73**, 3463 (1994).
[16] D. C. Johnston et al., Phys. Rev. B **35**, 219 (1987).
[17] M. Ogata, M.U. Luchini and T.M. Rice, Phys. Rev. B **44**, 12083 (1991).
[18] M. Imada, Phys. Rev. B **48**, 550 (1993), and references therein.
[19] M. Reigrotzki, H. Tsunetsugu and T.M. Rice, J. Phys: Cond. Matt. **6**, 9235 (1994); In Ref. 11 a term was omitted in the strong coupling expansion.
[20] Y. Nagaoka, Phys. Rev. **147**, 392 (1966); D.J. Thouless, Proc. Phys. Soc. **86**, 893 (1965).
[21] B. Doucot and X.G. Wen, Phys. Rev. B **40**, 2719 (1989).
[22] W. van der Linden and D.M. Edwards, J. Phys. Condens. Matter **3**, 4917 (1991); *ibid.* **3**, 7229 (1991); A.J. Basile and V. Elser, Phys. Rev. B **41**, 4842 (1990); B.S. Shastry, H.R. Krishnamurthy, and P.W. Anderson, Phys. Rev. B **41**, 2375 (1990).
[23] W.O. Putikka, M.U. Luchini and T.M. Rice, Phys. Rev. Lett. **68**, 538 (1992); W.O. Putikka, M.U. Luchini and M. Ogata, *ibid.* **69**, 2288 (1992).
[24] R. Hirsch, PhD thesis, Universität Köln; E. Müller-Hartmann, private communications.
[25] A. Luther and V.J. Emery, Phys. Rev. Lett. **33**, 589 (1974); V.J. Emery, in *Highly Conducting One-Dimensional Solids*, edited by J.T. Devreese et al. (Plenum, New York, 1979).
[26] F.D.M. Haldane, Phys. Rev. Lett. **45**, 1358 (1980); J. Phys. C **14**, 2585 (1981).
[27] M. Ogata, M.U. Luchini, S. Sorella and F.F. Assaad, Phys. Rev. Lett. **66**, 2388 (1991).
[28] Similar excitations are also found for a t-J chain with frustrated couplings: K. Takano and K. Sano, Phys. Rev. B **48**, 9831 (1993); I. Bose and S. Gayen, Phys. Rev. B **48**, 10653 (1993).
[29] V. Heine in *Solid State Physics*, Vol. 35, edited by H. Ehrenreich, F. Seitz and D. Turnbull (Academic Press, New York, 1980)
[30] R. Eder, Y. Ohta and S. Maekawa, Phys. Rev. Lett. **74**, 5124 (1995).
[31] T. Tohyama, P. Horsch and S. Maekawa, Phys. Rev. Lett. **74**, 980 (1995).
[32] K.B. Efetov and A.I. Larkin, Zh. Eksp. Teor. Fiz. **69**, 764 (1975) [Sov. Phys. JETP **42**, 390 (1976)].
[33] D. C. Mattis and E. H. Lieb, J. Math. Phys. **6**, 304 (1965).
[34] A. Luther and I. Peschel, Phys. Rev. B **9**, 2911 (1974); ibid. B **12**, 3908 (1975)
[35] H. J. Schulz, Phys. Rev. Lett. **64**, 2831 (1990); Int. J. Mod. Phys. B **5**, 57 (1991); B. S. Shastry and B. Sutherland, Phys. Rev. Lett. **65**, 243 (1990).
[36] C. A. Hayward et al., *Evidence for a superfluid density in t-J ladders*, preprint cond-mat/9504018.
[37] D. S. Dessau et al., Phys. Rev. Lett. **71**, 2781 (1993).
[38] W. Stephan and P. Horsch, Phys. Rev. Lett. **66**, 2258 (1991).
[39] Y. Ohta, T. Shimozato, R. Eder and S. Maekawa, Phys. Rev. Lett. **73**, 324 (1994).

TABLE I. Parameters for the fit of the lowest lying bands of the one-hole spectra to a dispersion of the form of Eq. (15).

J/t	k_y	ΔE	α_1	α_2	α_3
0.3	0	−1.476	0.160	0.103	−0.026
0.3	π	−1.417	−0.192	0.134	0.025
0.5	0	−0.865	0.263	0.189	−0.007
0.5	π	−0.790	−0.311	0.225	−0.011

FIG. 1. The t-J ladder with two legs and L rungs. The couplings along the legs are t, J and those along the rungs t', J'.

FIG. 2. Ground state energies for the t ladder (t-J ladder with $J = J' = 0$) with two holes. Results are shown for systems with $L = 2, 3, \ldots, 10$ rungs and periodic (PBC) as well as antiperiodic (APBC) boundary conditions. The ferromagnetic state always has the lowest energy for $L \geq 4$ rungs.

FIG. 3. Real-space spin correlations for the singlet ground state of the t ladder with two holes. $L = 10$ and PBC's are used. The two ferromagnetic domains can clearly be seen.

FIG. 4. Graphical representation of the low-lying states of the t-J ladder in the strong coupling limit $J' \gg J, t$. (a) The undoped case. (b) One hole goes into either the bonding orbital or the antibonding orbital on one rung. (c) In the ground state for two holes both holes are on the same rung. (d) Scattering states of two holes. (e) At higher energies there is the triplet excitation similar to the undoped ladder.

FIG. 5. Binding energy of two holes, spin gap and energy of the triplet excitation away from the bound hole pair. $J/t = 0.3$ and $0.3 \leq J'/t \leq 3.0$. The size of the ladder is $L = 8$ rungs.

FIG. 6. Hole-hole correlation functions for the ground state of the t-J ladder with two holes. $J/t = 0.3$, and J'/J=1 and 10. The size of the ladder is $L = 10$ rungs and APBC's are used, which have a lower ground state energy than PBC's. The inset shows the size of the bound hole pair, ξ, in the two-hole ground state as a function of J' for different ladder sizes.

FIG. 7. The line of phase separation in the t-J ladder determined from the coupling at which the compressibility diverges.

FIG. 8. The nine different states for a single rung.

FIG. 9. Energy spectra for the t-J ladder doped with one hole. The case of large J' ($J'/J = 10$): (a) $J/t = 0.3$ and (b) $J/t = 0.5$ with $L = 8$. The isotropic case ($J'/J = 1$): (c) $J/t = 0.3$ and (d) $J/t = 0.5$ with $L = 10$. The results for $k_x = \frac{n}{L}\pi$ with even n are for PBC's and with odd n for APBC's.

FIG. 10. Fit of the lowest lying bands of the one-hole spectra to the form of Eq. (15). (a) $J/t = J'/t = 0.3$ and (b) $J/t = J'/t = 0.5$. The size is $L = 10$.

FIG. 11. The hole-spin correlations for the ground state of the ladder doped with one hole at $J'/J = 1$and 10. The ladder has $L = 10$ rungs and $J/t = 0.3$. The ground state has $S^z = 1/2$.

FIG. 12. Energy spectra for the t-J ladder doped with two holes for a large J' ($J'/J = 10$): $J/t = 0.3$ with (a) PBC's and (b) APBC's, and $J/t = 0.5$ with (c) PBC's and (d) APBC's. The size of the ladder is $L = 8$ rungs. The states are classified according to total spin S and parity.

FIG. 13. Energy spectra for the t-J ladder doped with two holes at the isotropic point ($J'/J = 1$): $J/t = 0.3$ with (a) PBC's and (b) APBC's, and $J/t = 0.5$ with (c) PBC's and (d) APBC's. The size of the ladder is $L = 10$ rungs. The lines are only guides for the eye and do not necessarily connect related states.

FIG. 14. Hole-hole [(a) and (c)] and spin-hole [(b) and (d)] correlation functions for the two triplet excitations. $L = 8$. Dashed lines are for the lowest triplet state and dashed-dotted lines for the lowest state with non-vanishing weight in $\mathcal{S}(\mathbf{q} = (\pi, \pi), \omega)$.

FIG. 15. Dynamical spin structure factor, $\mathcal{S}(\mathbf{q}, \omega)$, for the undoped ladder with $L = 10$ rungs. Note that the scale is different for $q_y = \pi$.

FIG. 16. Dynamical spin structure factor, $\mathcal{S}(\mathbf{q}, \omega)$, for the $L = 10$ ladder with two holes. $J/t = J'/t = 0.3$ (upper panels) and 0.5 (lower panels). PBC's are used. Note that the scale is different for around $\mathbf{q} = (\pi, \pi)$.

FIG. 17. Dynamical charge structure factor, $\mathcal{N}(\mathbf{q}, \omega)$, for the $L = 10$ ladder with two holes. $J/t = J'/t = 0.3$ (upper panels) and 0.5 (lower panels). PBC's are used.

FIG. 18. Superconducting order parameter, $\chi_{\mathbf{k}}$ for $N_{\rm h} = 2$ calculated on the $L = 8$ ladder with PBC's for several values of $J/t = J'/t$.

FIG. 19. The order parameter for the optimal pair Eq. (27) as a function of J/t on an $L = 8$ ladder with both PBC and APBC. Shown are results for 2 and 4 holes.

FIG. 20. Correlation exponent, K_ρ, for the $L = 7$ ladder with two holes.

FIG. 21. Spectral function of the one-particle Green's function, $A(\mathbf{k},\omega)$, for the $L = 10$ ladder with two holes. (a) $J/t = J'/t = 0.3$ and (b) $J/t = J'/t = 0.5$. The width of each line represents the strength of the excitation. For $\omega > 0$ we show the spectral function for *adding* one electron $A_{\mathrm{e},\sigma}(\mathbf{k},\omega)$, and for $\omega < 0$ the spectral function for *removing* an electron $A_{\mathrm{h},\sigma}(\mathbf{k},\omega)$.

FIG. 22. Spectral function of the one-particle Green's function for two holes summed over all wave vectors; $A_{\mathrm{h},\sigma}(\omega)$ $=\sum_{\mathbf{k}} A_{h,\sigma}(\mathbf{k},\omega)$ and $A_{\mathrm{e},\sigma}(\omega)= \sum_{\mathbf{k}} A_{\mathrm{e},\sigma}(\mathbf{k},\omega)$. $L = 10$ and $J/t = J'/t = 0.3$. The oscillations at large $|\omega|$ are caused by nonconvergent Lanczos iterations at these energies.

FIG. 23. The momentum distribution function for the ground state for $\delta = 0.1$ and $L = 10$. $J/t = J'/t = 0.3$. The electron part, $n^{\mathrm{e}}_{\sigma}(\mathbf{k})= \langle c^{\dagger}_{\mathbf{k},\sigma} c_{\mathbf{k},\sigma}\rangle$, and the hole part, $n^{\mathrm{h}}_{\sigma}(\mathbf{k})= \langle c_{\mathbf{k},\sigma} c^{\dagger}_{\mathbf{k},\sigma}\rangle$. The momenta, $k_x = 2\pi n/L$, with integer n's are for PBC's, while those with half-integer n's are for APBC's.

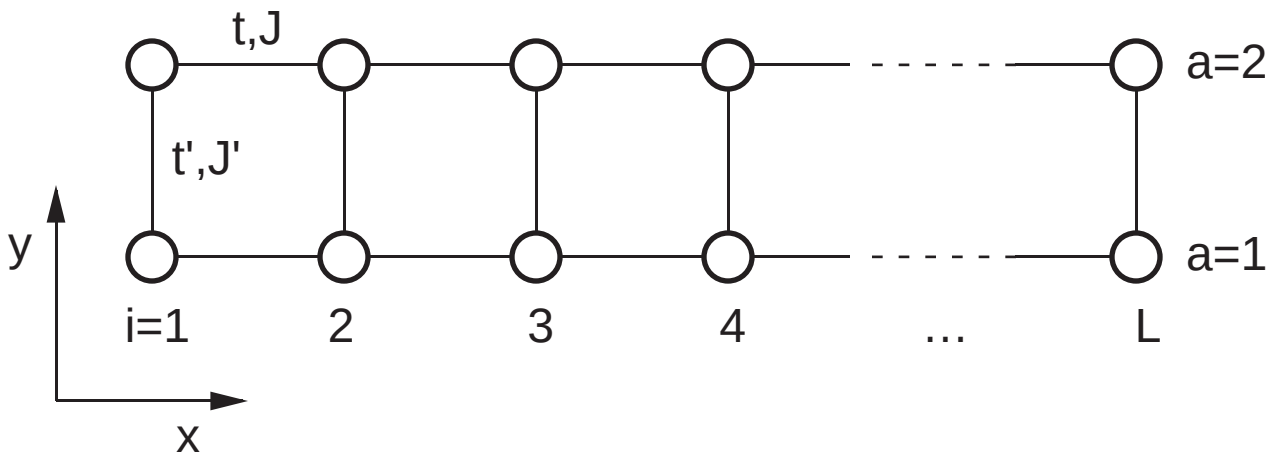
t,J
t',J'
a=2
a=1
y
x
i=1
2
3
4
…
L

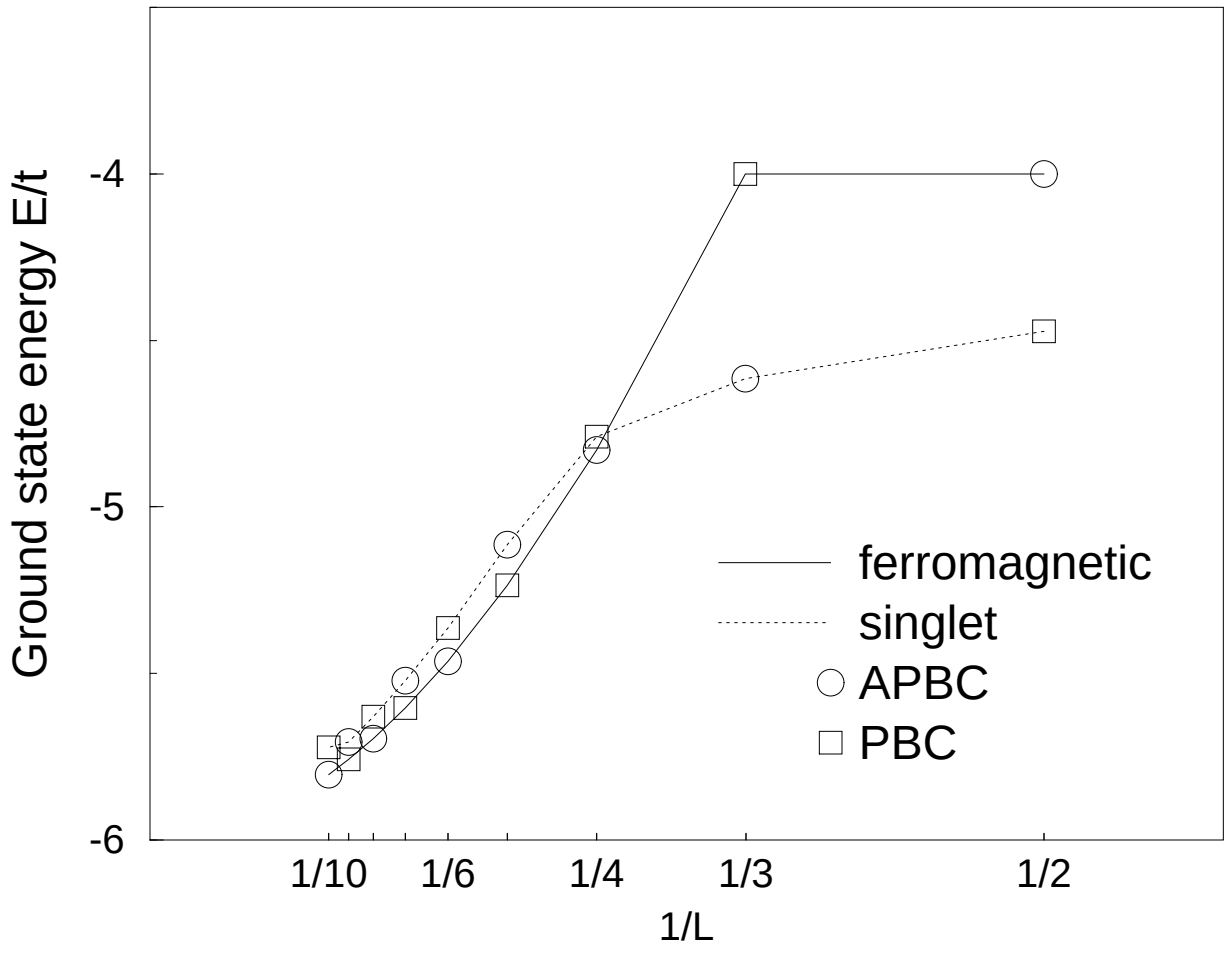
Ground state energy E/t
-4
-5
-6
1/10
1/6
1/4
1/3
1/2
1/L
ferromagnetic
singlet
APBC
PBC

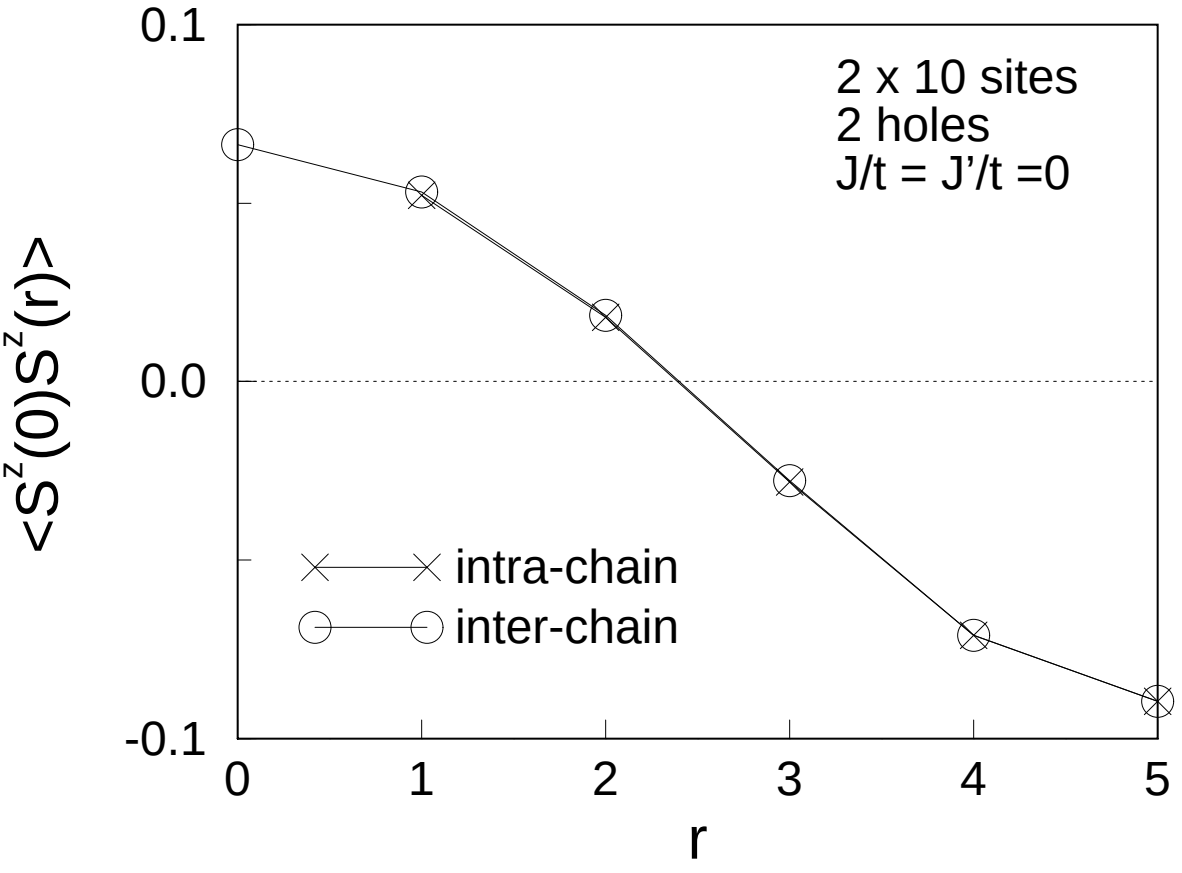
0.1
0.0
-0.1
0
1
2
3
4
5
r
<S^z(0)S^z(r)>
2 x 10 sites
2 holes
J/t = J'/t =0
intra-chain
inter-chain

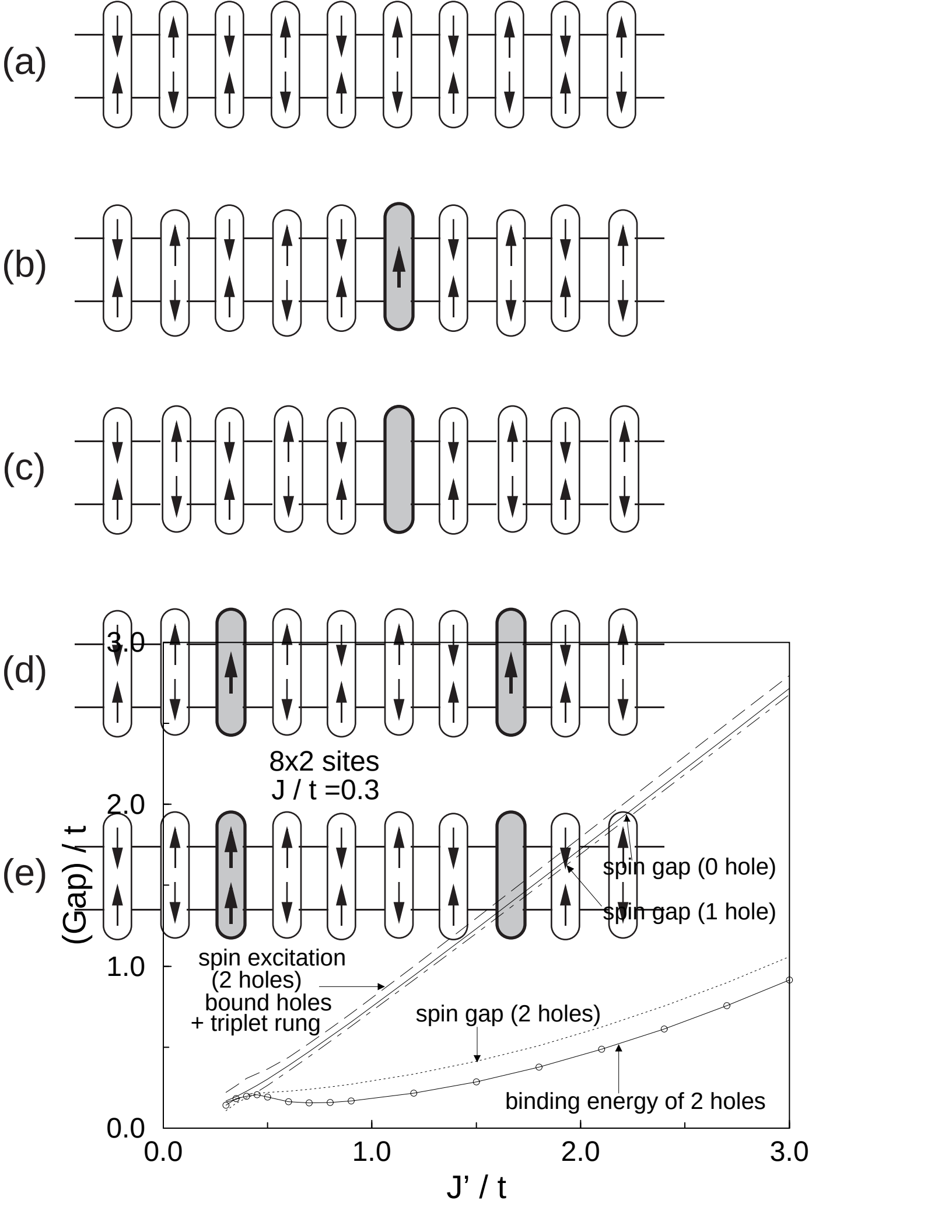
(a)
(b)
(c)
(d)
(e)
8x2 sites
J / t =0.3
(Gap) / t
J' / t
0.0
1.0
2.0
3.0
spin gap (0 hole)
spin gap (1 hole)
spin excitation
(2 holes)
bound holes
+ triplet rung
spin gap (2 holes)
binding energy of 2 holes

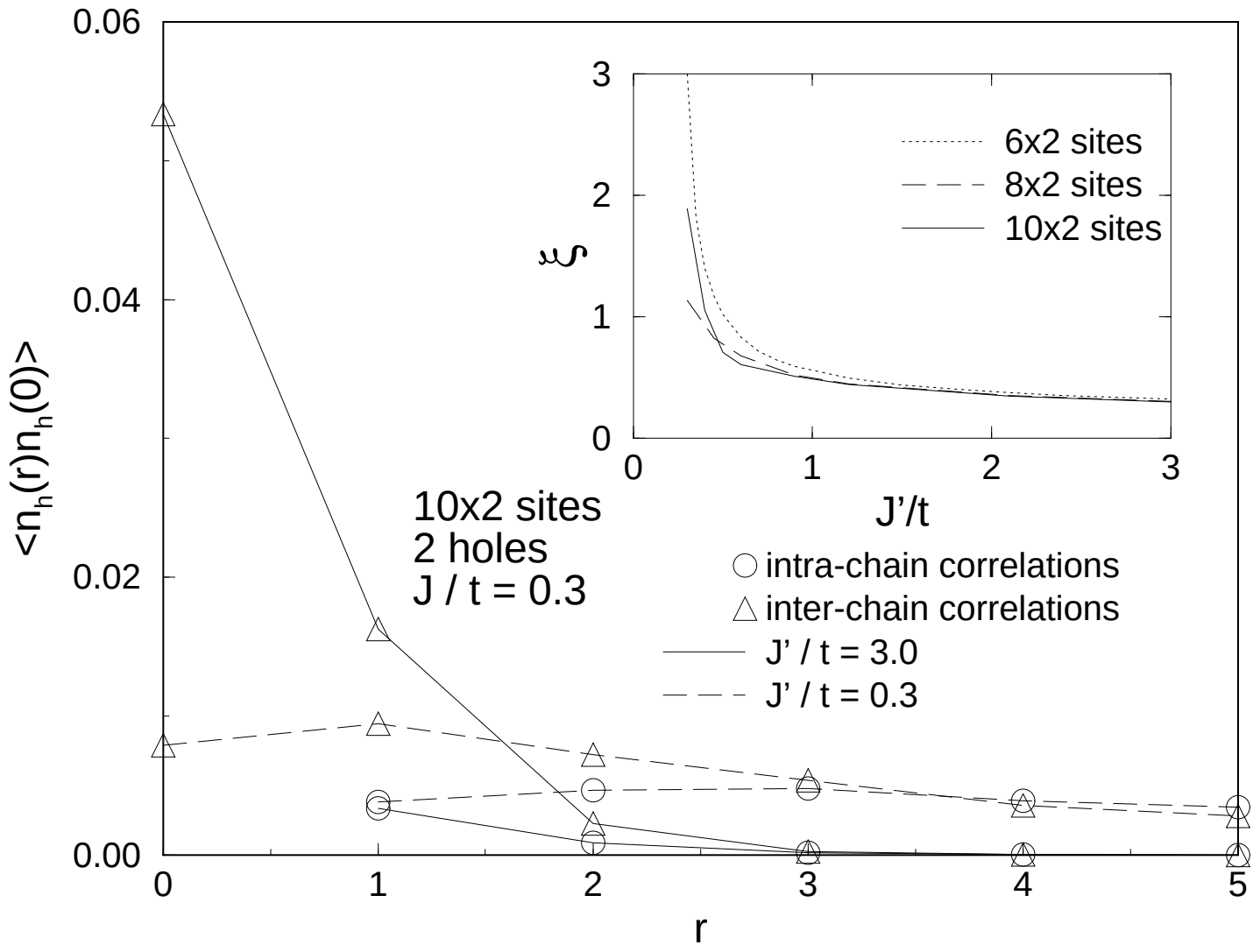
0.06
0.04
0.02
0.00
0
1
2
3
4
5
r
<n_h(r)n_h(0)>
10x2 sites
2 holes
J / t = 0.3
intra-chain correlations
inter-chain correlations
J' / t = 3.0
J' / t = 0.3
3
2
1
0
0
1
2
3
J'/t
6x2 sites
8x2 sites
10x2 sites

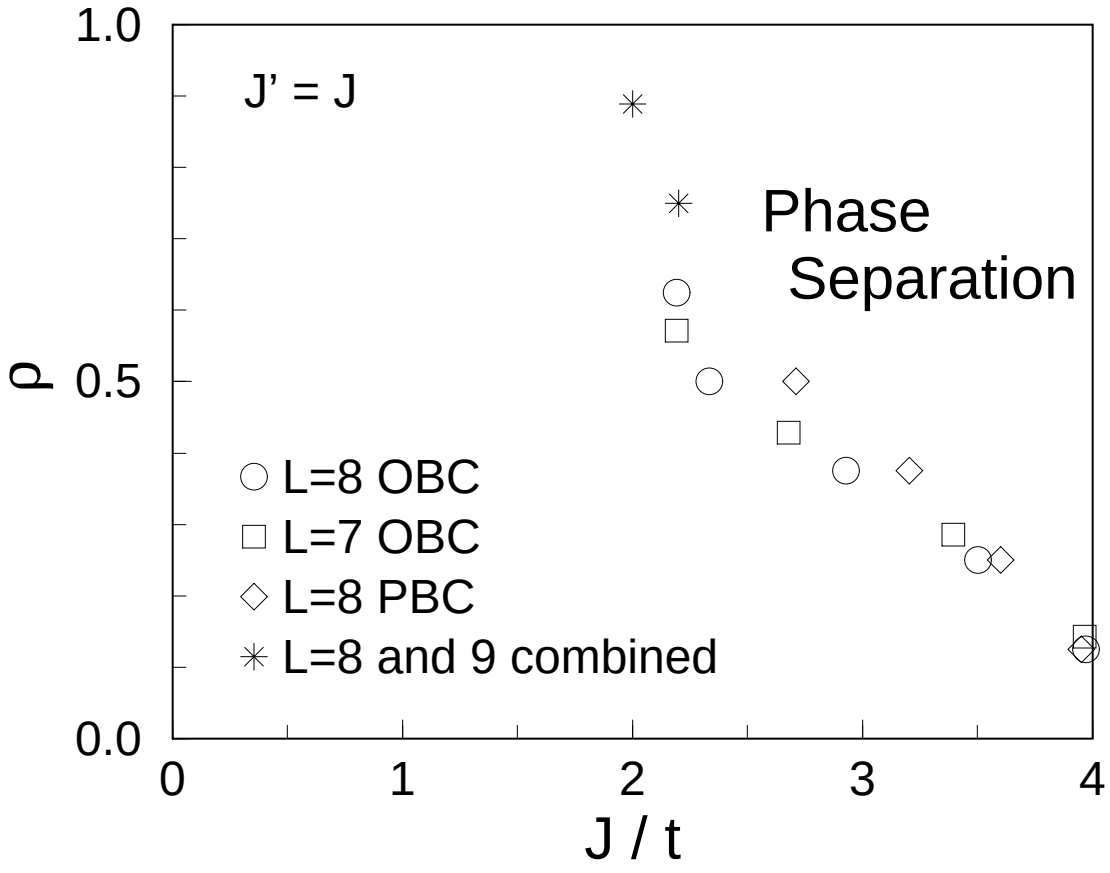
1.0
0.5
0.0
ρ
J' = J
Phase
Separation
L=8 OBC
L=7 OBC
L=8 PBC
L=8 and 9 combined
0
1
2
3
4
J / t

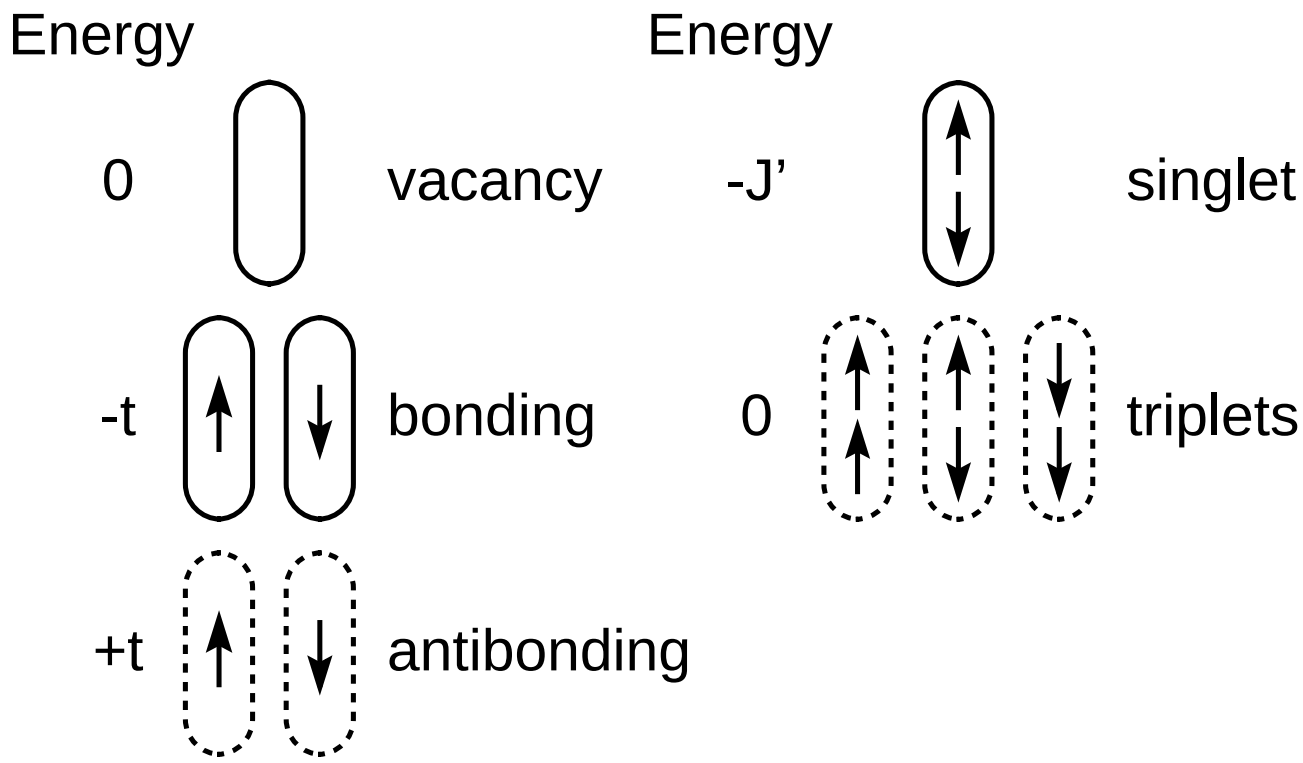
Energy
0
vacancy
-t
bonding
+t
antibonding
Energy
-J’
singlet
0
triplets

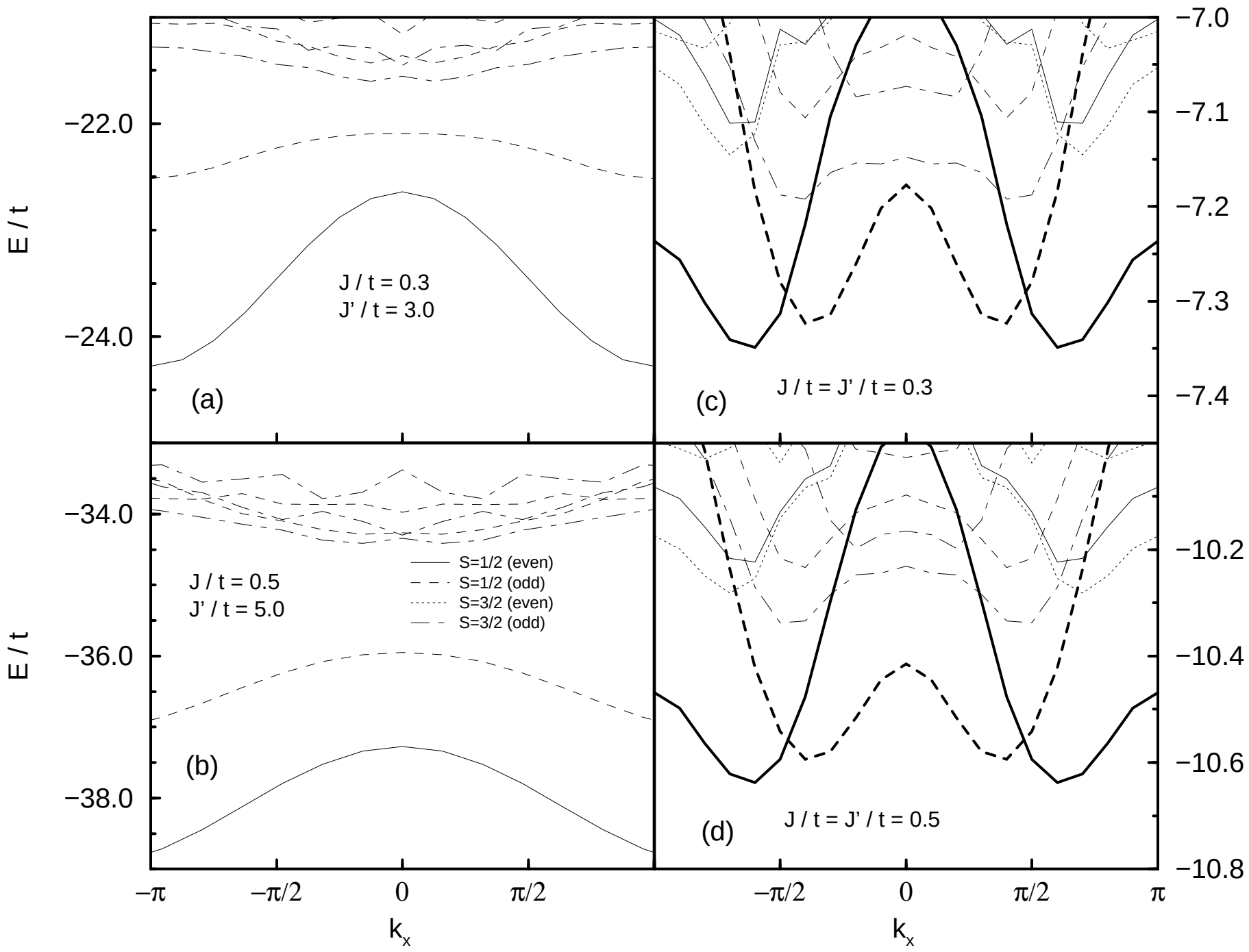
E / t
−22.0
−24.0
J / t = 0.3
J' / t = 3.0
(a)
−7.0
−7.1
−7.2
−7.3
−7.4
J / t = J' / t = 0.3
(c)
−34.0
−36.0
−38.0
J / t = 0.5
J' / t = 5.0
S=1/2 (even)
S=1/2 (odd)
S=3/2 (even)
S=3/2 (odd)
(b)
−10.2
−10.4
−10.6
−10.8
J / t = J' / t = 0.5
(d)
−π
−π/2
0
π/2
π
k_x

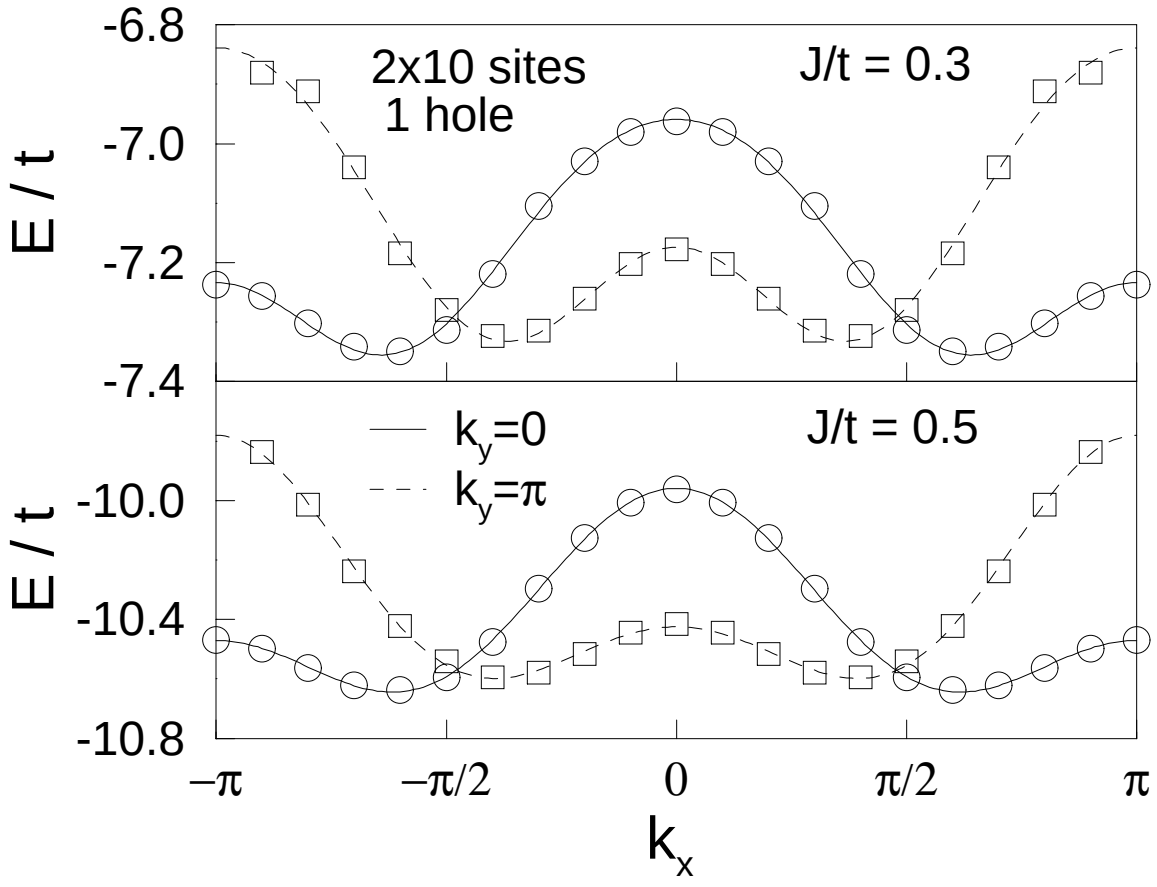
-6.8
-7.0
-7.2
-7.4
E / t
2x10 sites
1 hole
J/t = 0.3
k_y=0
k_y=π
J/t = 0.5
-10.0
-10.4
-10.8
E / t
–π
–π/2
0
π/2
π
k_x

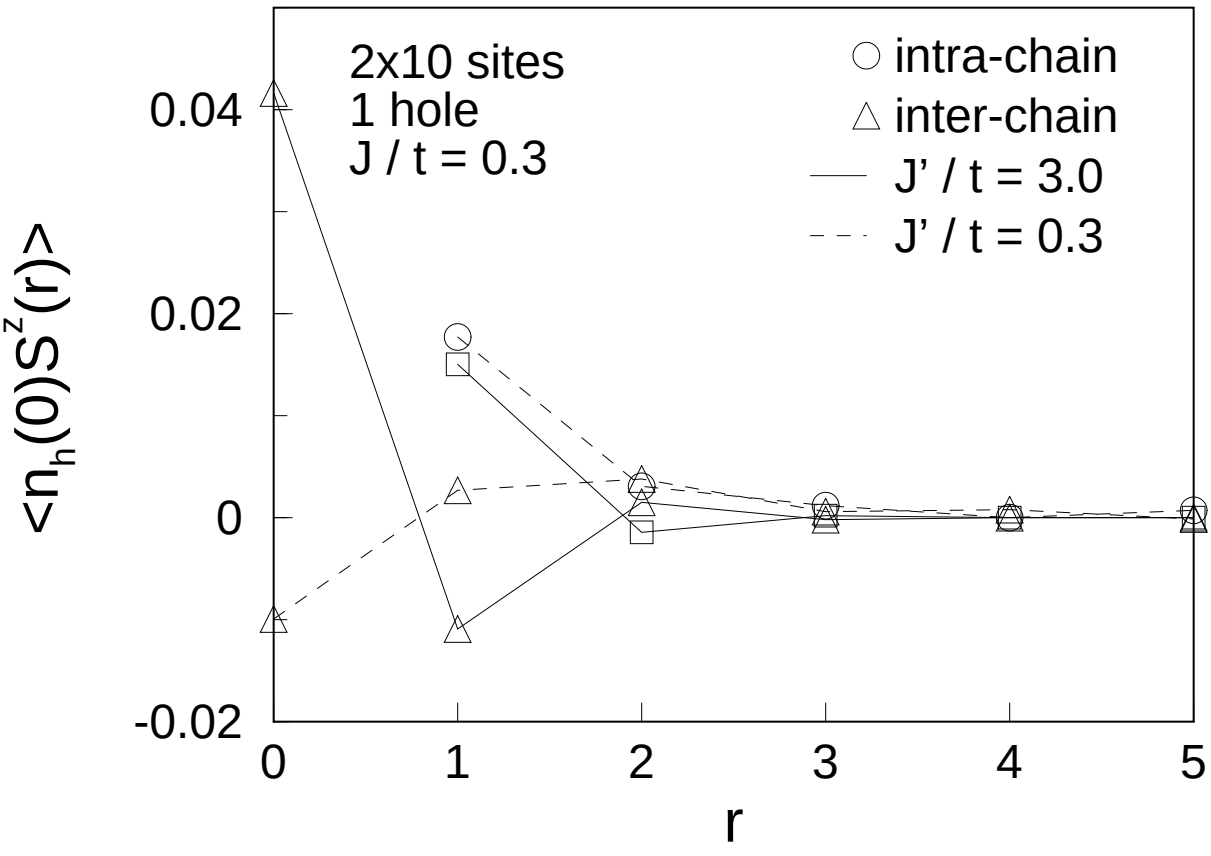
2x10 sites
1 hole
J / t = 0.3
intra-chain
inter-chain
J' / t = 3.0
J' / t = 0.3
0.04
0.02
0
-0.02
0
1
2
3
4
5
r
<n_h(0)S^z(r)>

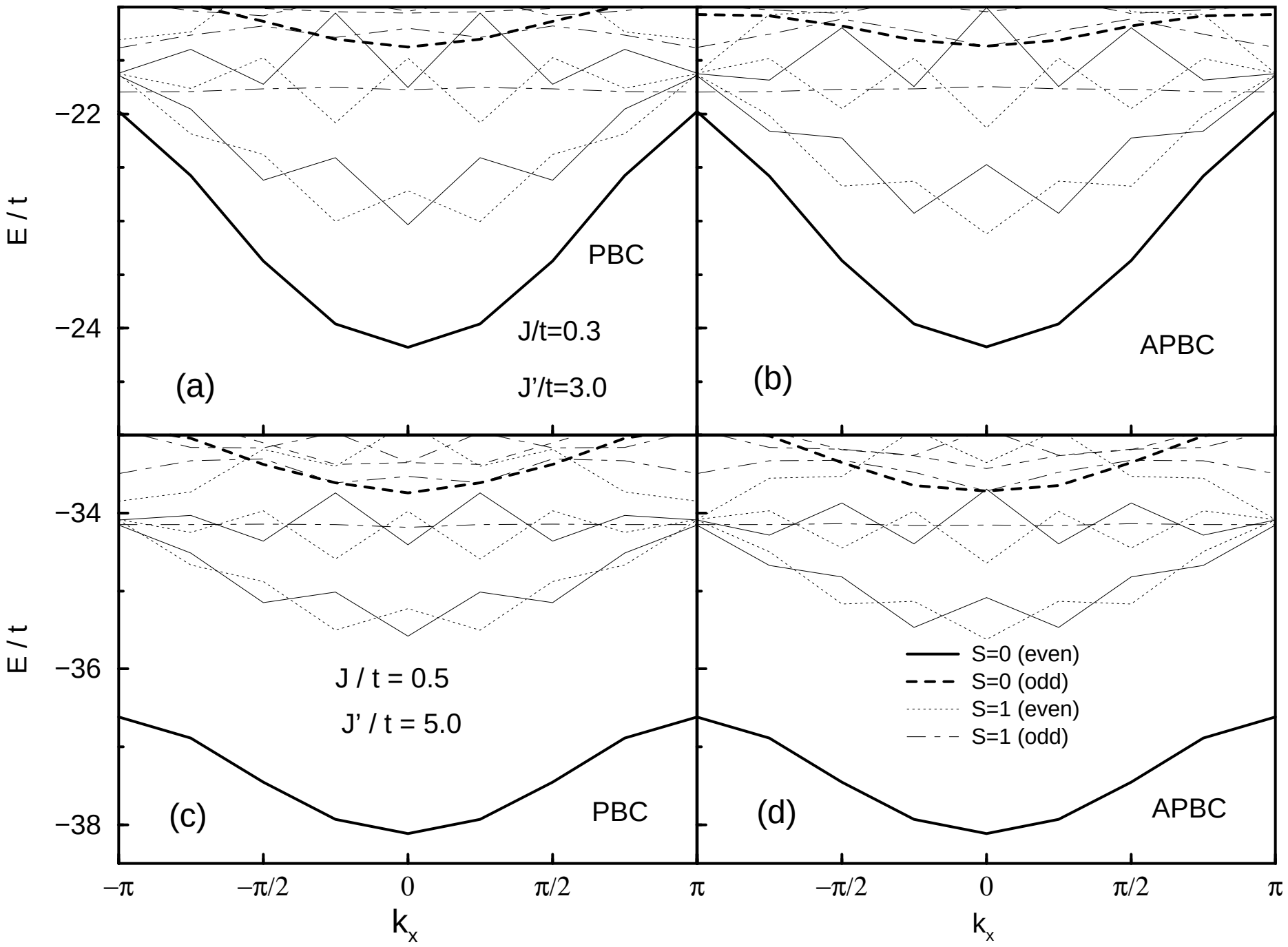
E / t
−22
−24
−34
−36
−38
PBC
J/t=0.3
J'/t=3.0
(a)
(b)
APBC
J / t = 0.5
J' / t = 5.0
(c)
(d)
S=0 (even)
S=0 (odd)
S=1 (even)
S=1 (odd)
−π
−π/2
0
π/2
π
k_x

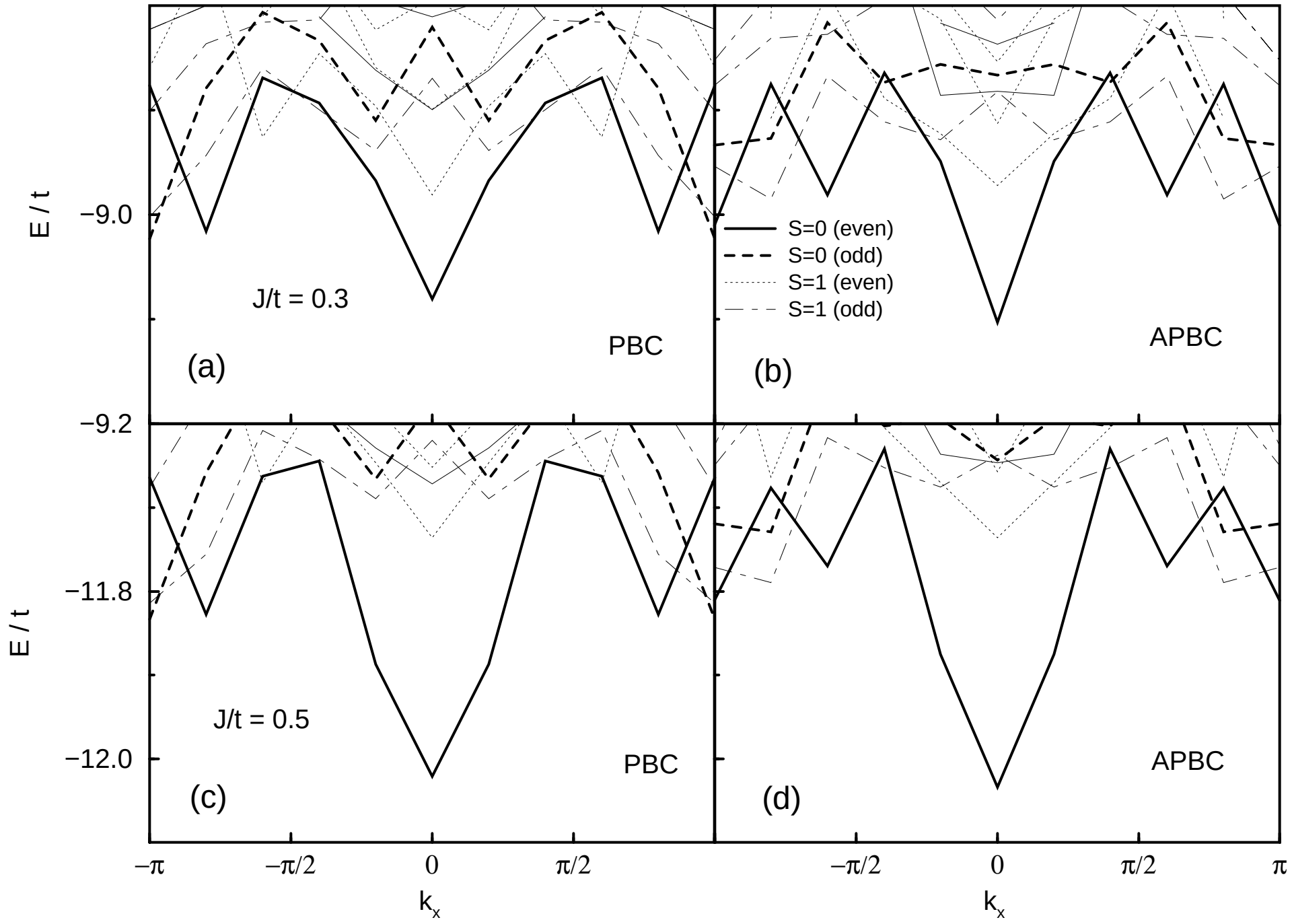
E / t
−9.0
−9.2
−11.8
−12.0
J/t = 0.3
PBC
(a)
S=0 (even)
S=0 (odd)
S=1 (even)
S=1 (odd)
APBC
(b)
J/t = 0.5
PBC
(c)
APBC
(d)
−π
−π/2
0
π/2
π
k_x

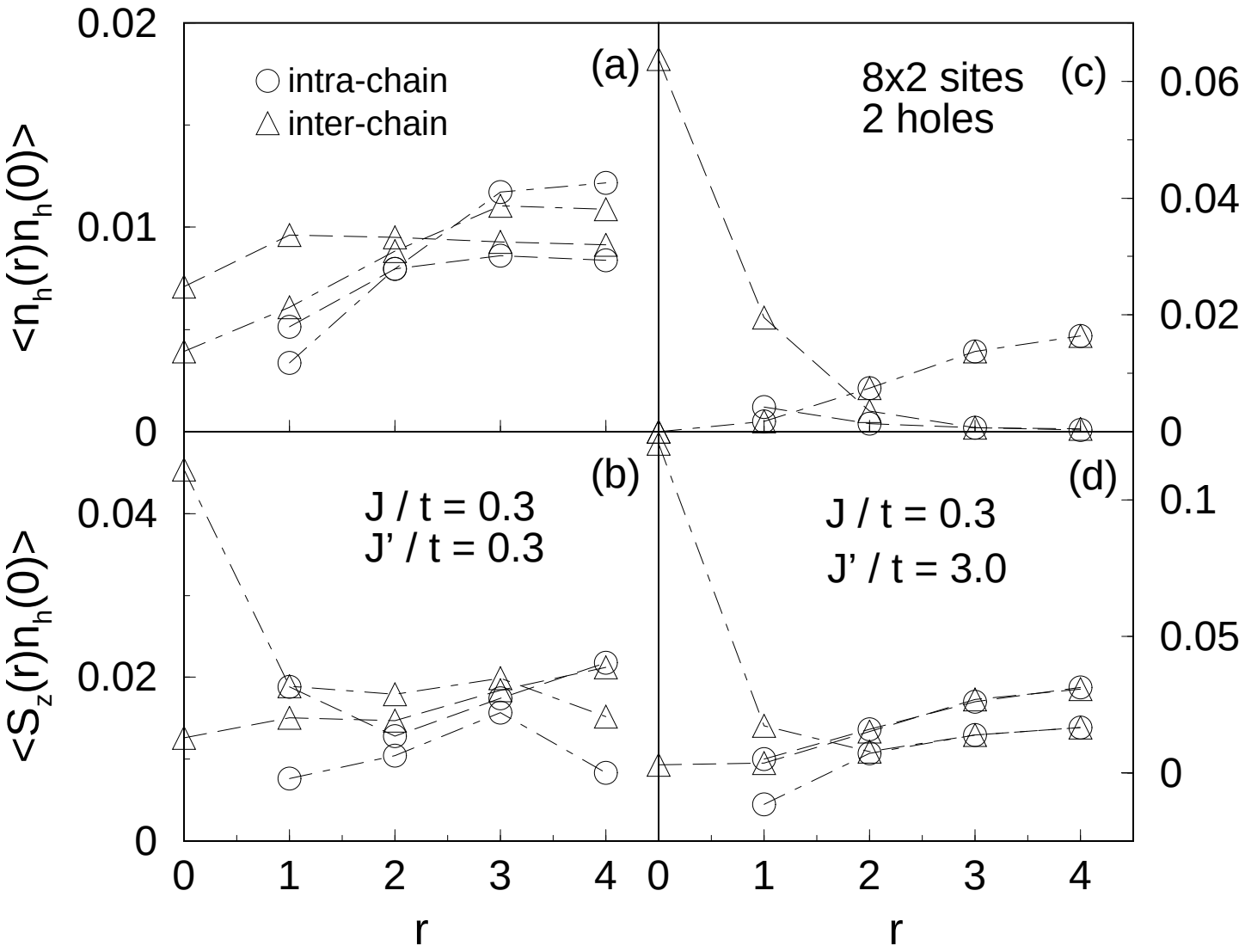
intra-chain
inter-chain
(a)
(b)
(c)
(d)
8x2 sites
2 holes
J / t = 0.3
J' / t = 0.3
J / t = 0.3
J' / t = 3.0
<n_h(r)n_h(0)>
<S_z(r)n_h(0)>
r
r
0.02
0.01
0
0.04
0.02
0
0.06
0.04
0.02
0
0.1
0.05
0
0
1
2
3
4

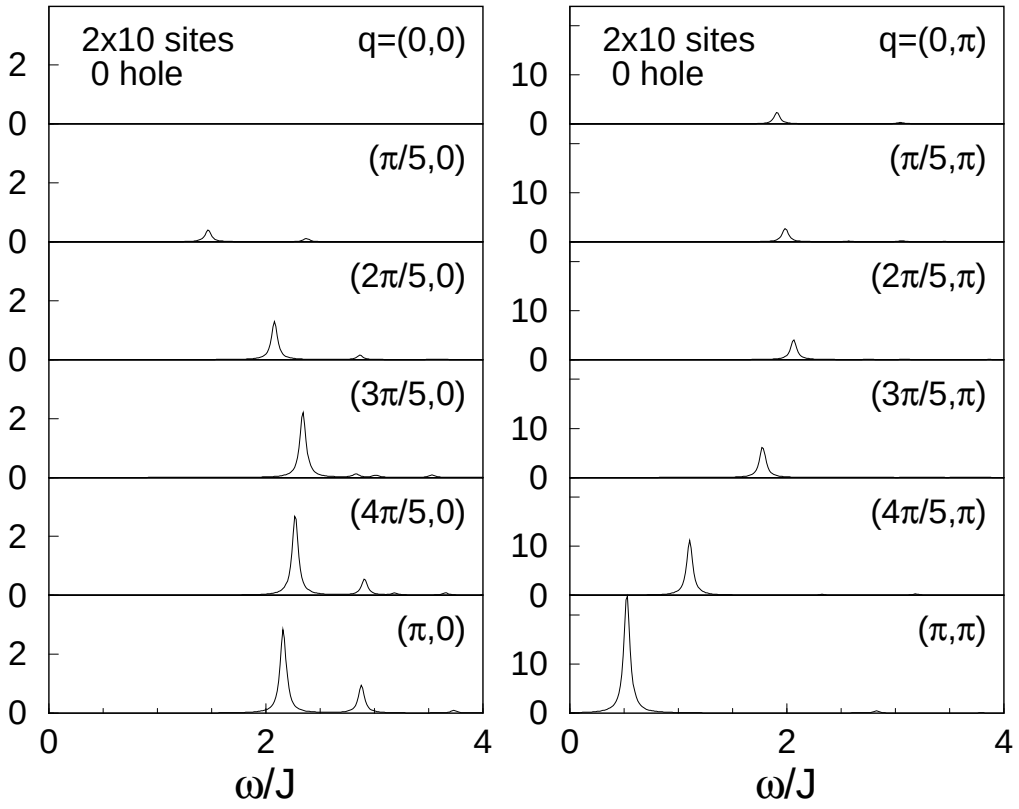
2x10 sites
0 hole
q=(0,0)
(π/5,0)
(2π/5,0)
(3π/5,0)
(4π/5,0)
(π,0)
2x10 sites
0 hole
q=(0,π)
(π/5,π)
(2π/5,π)
(3π/5,π)
(4π/5,π)
(π,π)
ω/J
ω/J

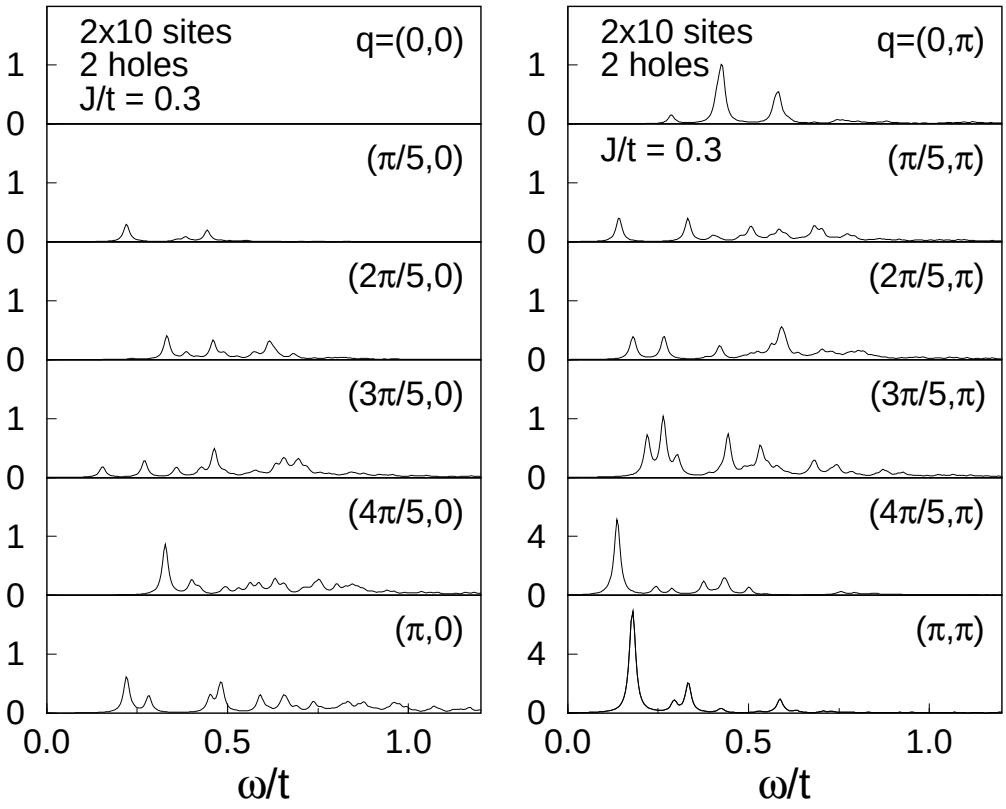
2x10 sites
2 holes
J/t = 0.3
q=(0,0)
(π/5,0)
(2π/5,0)
(3π/5,0)
(4π/5,0)
(π,0)
q=(0,π)
(π/5,π)
(2π/5,π)
(3π/5,π)
(4π/5,π)
(π,π)
ω/t

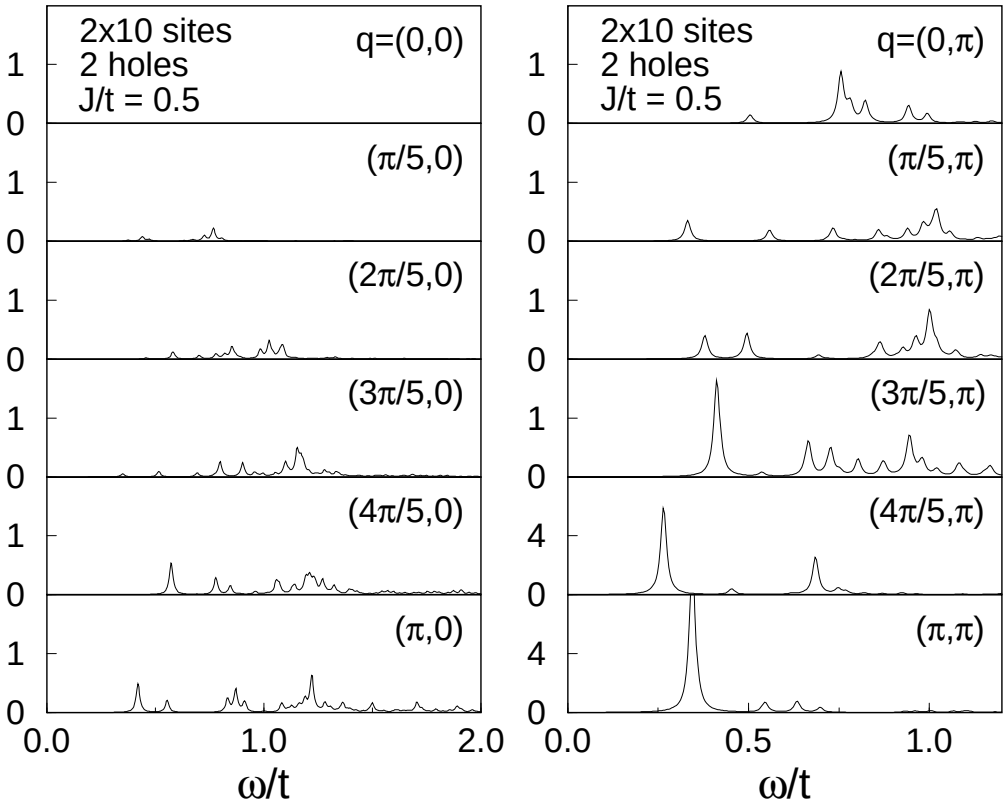
2x10 sites
2 holes
J/t = 0.5
q=(0,0)
(π/5,0)
(2π/5,0)
(3π/5,0)
(4π/5,0)
(π,0)
q=(0,π)
(π/5,π)
(2π/5,π)
(3π/5,π)
(4π/5,π)
(π,π)
ω/t

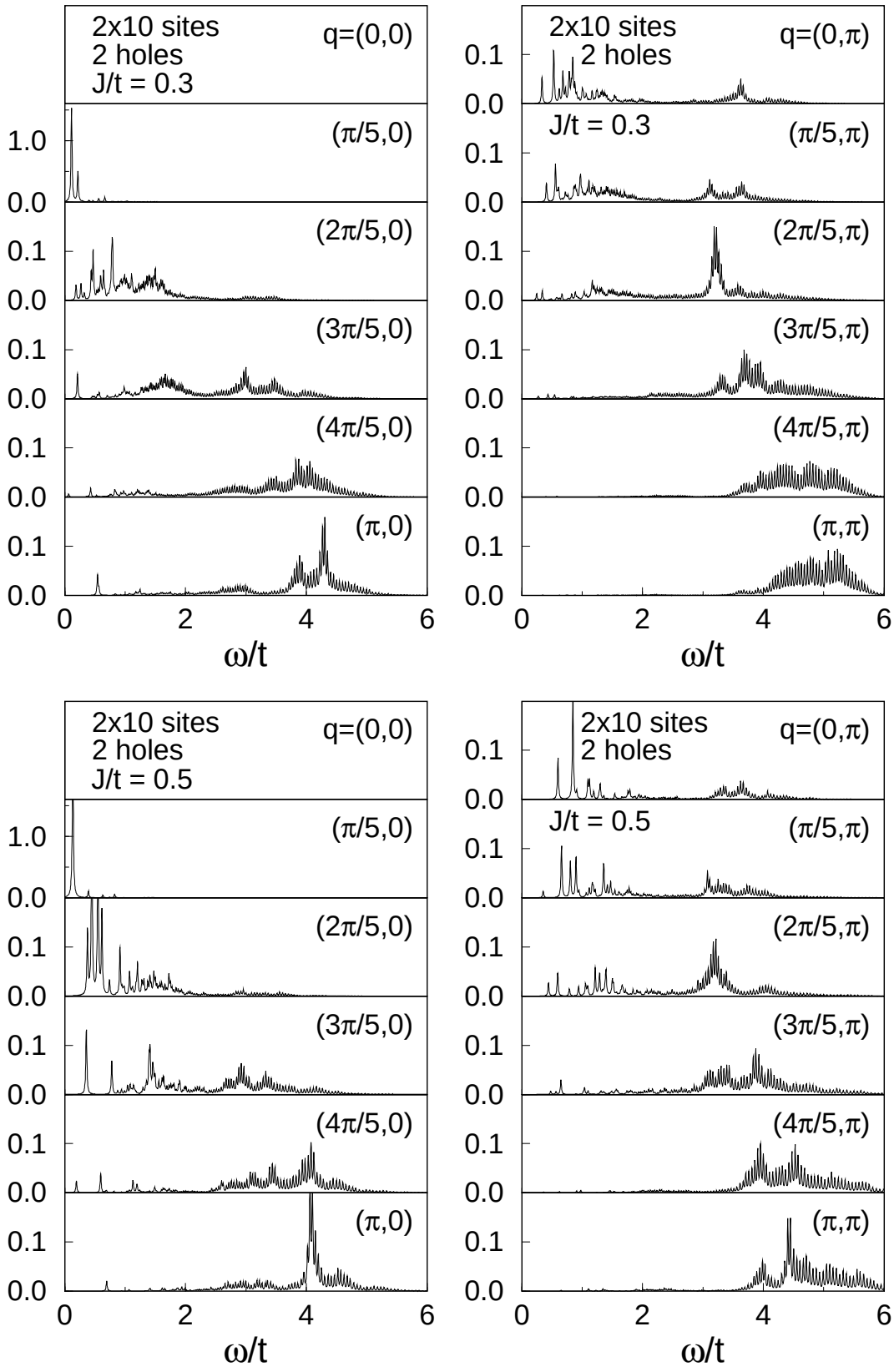
2x10 sites
2 holes
J/t = 0.3
q=(0,0)
(π/5,0)
(2π/5,0)
(3π/5,0)
(4π/5,0)
(π,0)
q=(0,π)
(π/5,π)
(2π/5,π)
(3π/5,π)
(4π/5,π)
(π,π)
1.0
0.1
0.0
0
2
4
6
ω/t
2x10 sites
2 holes
J/t = 0.5
q=(0,0)
(π/5,0)
(2π/5,0)
(3π/5,0)
(4π/5,0)
(π,0)
q=(0,π)
(π/5,π)
(2π/5,π)
(3π/5,π)
(4π/5,π)
(π,π)
ω/t

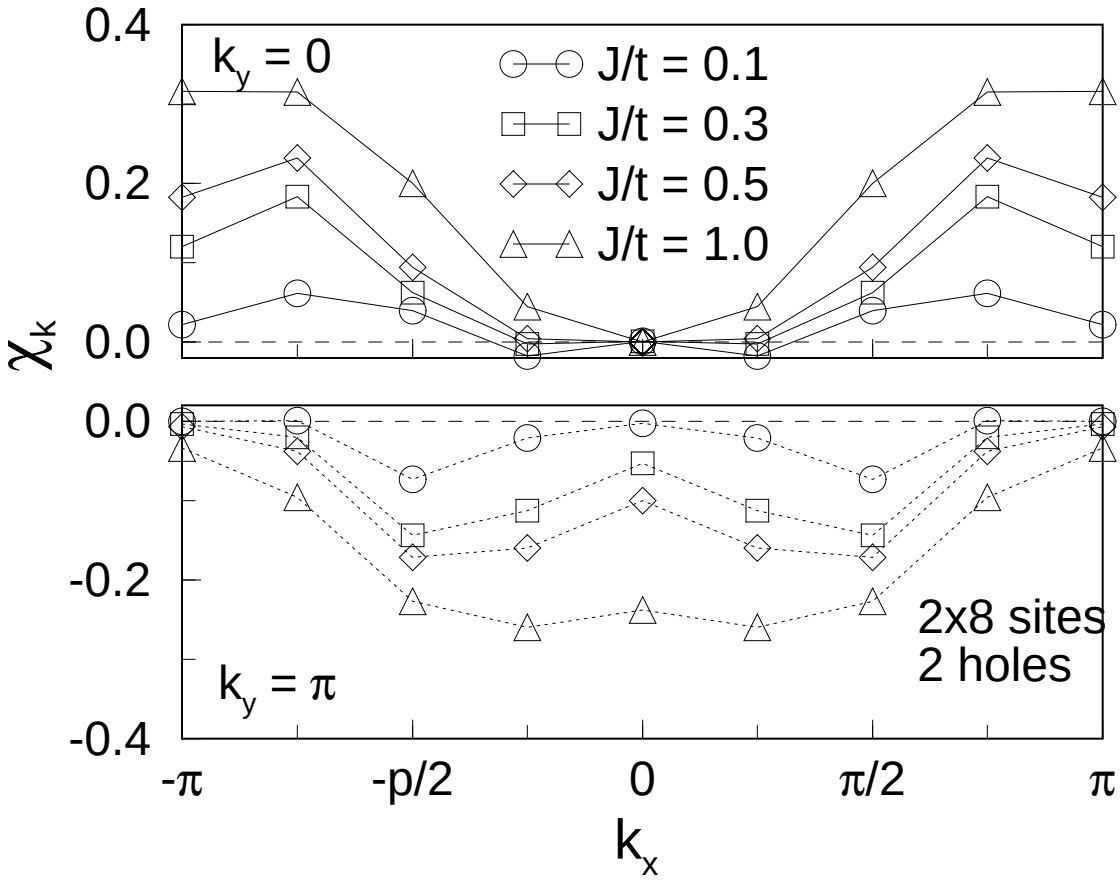
0.4
0.2
0.0
0.0
-0.2
-0.4
χ_k
$k_y = 0$
J/t = 0.1
J/t = 0.3
J/t = 0.5
J/t = 1.0
$k_y = \pi$
2x8 sites
2 holes
-π
-p/2
0
π/2
π
k_x

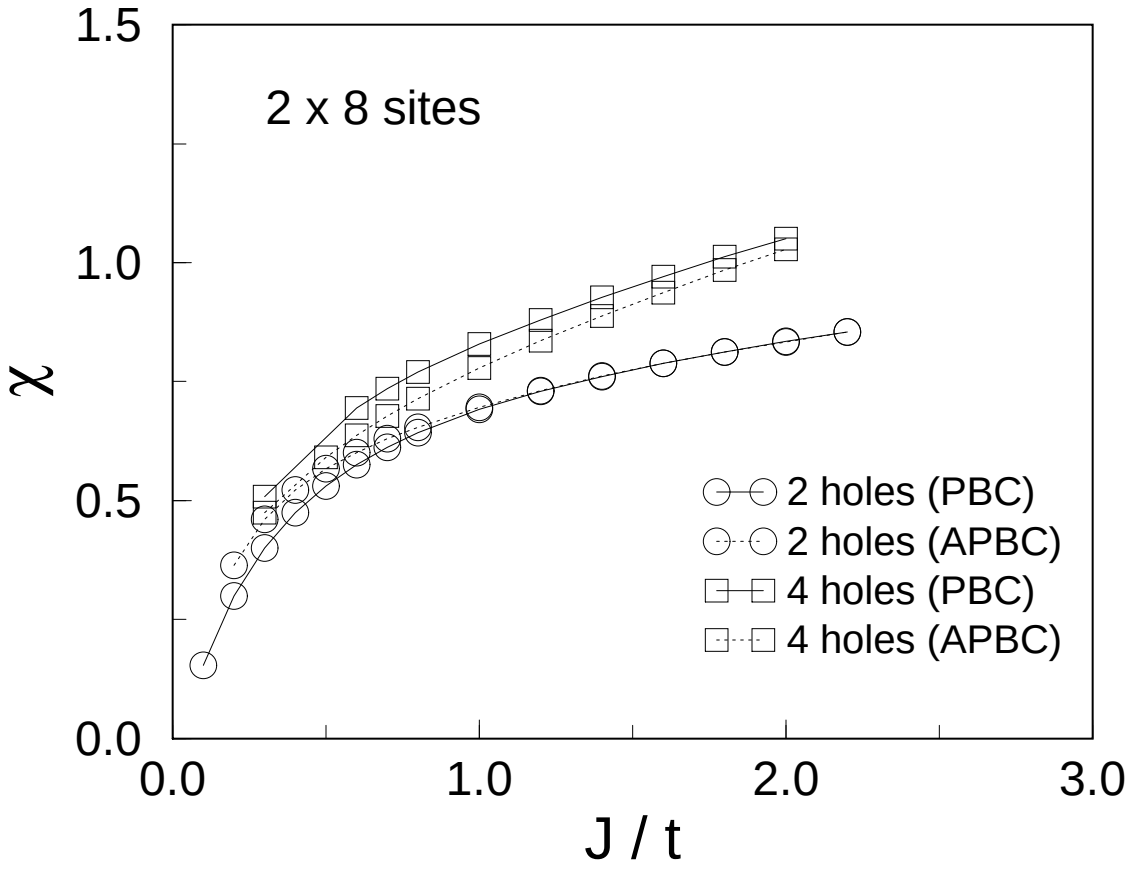
2 x 8 sites
χ
J / t
0.0
0.5
1.0
1.5
0.0
1.0
2.0
3.0
2 holes (PBC)
2 holes (APBC)
4 holes (PBC)
4 holes (APBC)

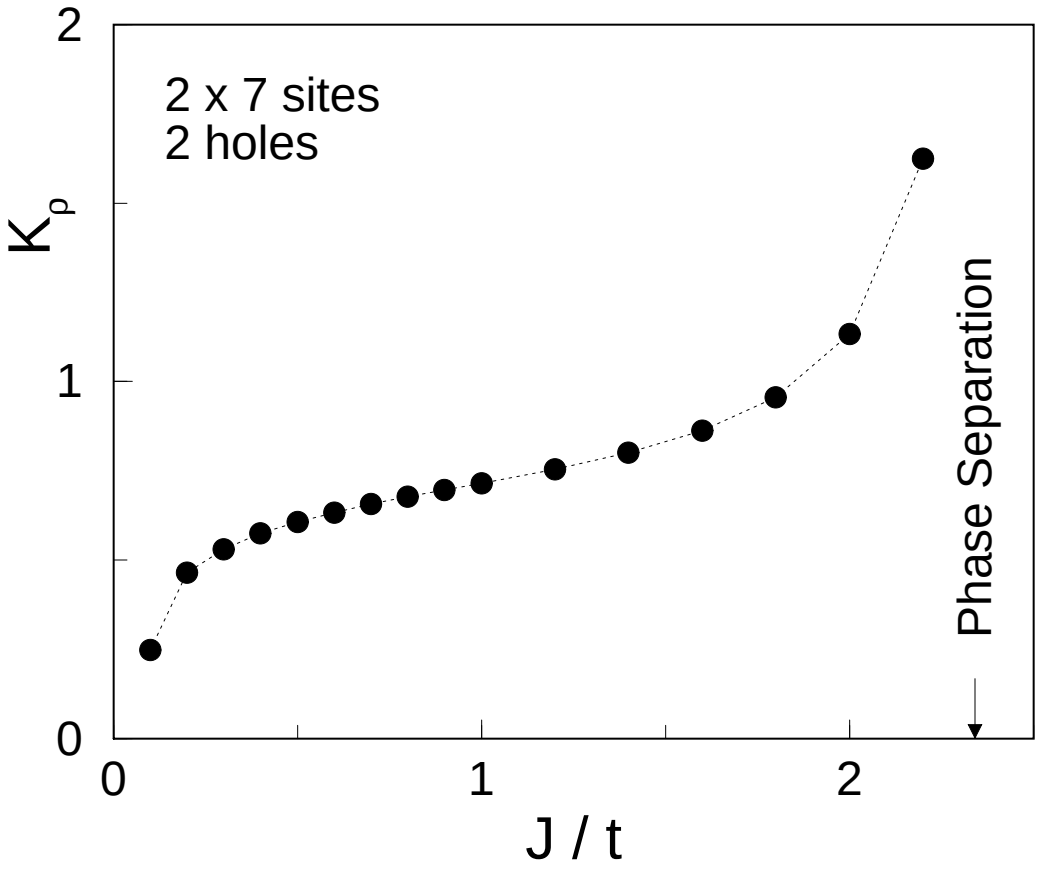
2 x 7 sites
2 holes
K_ρ
2
1
0
0
1
2
J / t
Phase Separation

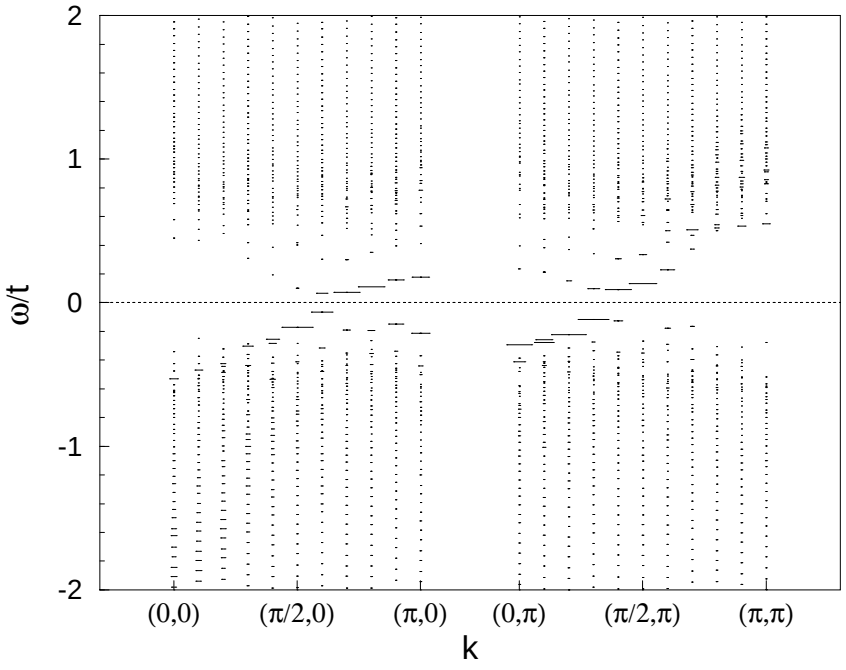
2
1
0
-1
-2
ω/t
(0,0)
(π/2,0)
(π,0)
(0,π)
(π/2,π)
(π,π)
k

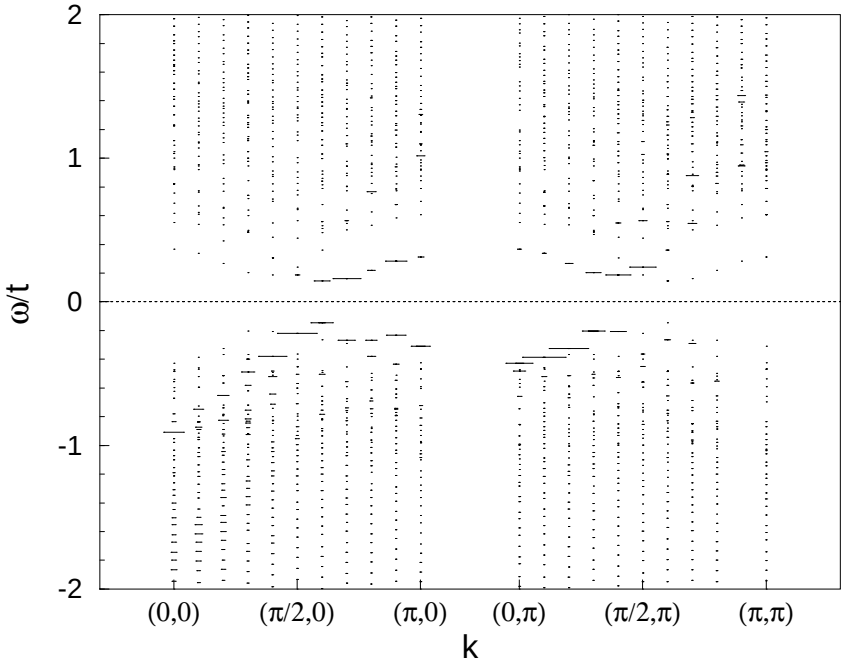
2
1
0
-1
-2
ω/t
(0,0)
(π/2,0)
(π,0)
(0,π)
(π/2,π)
(π,π)
k

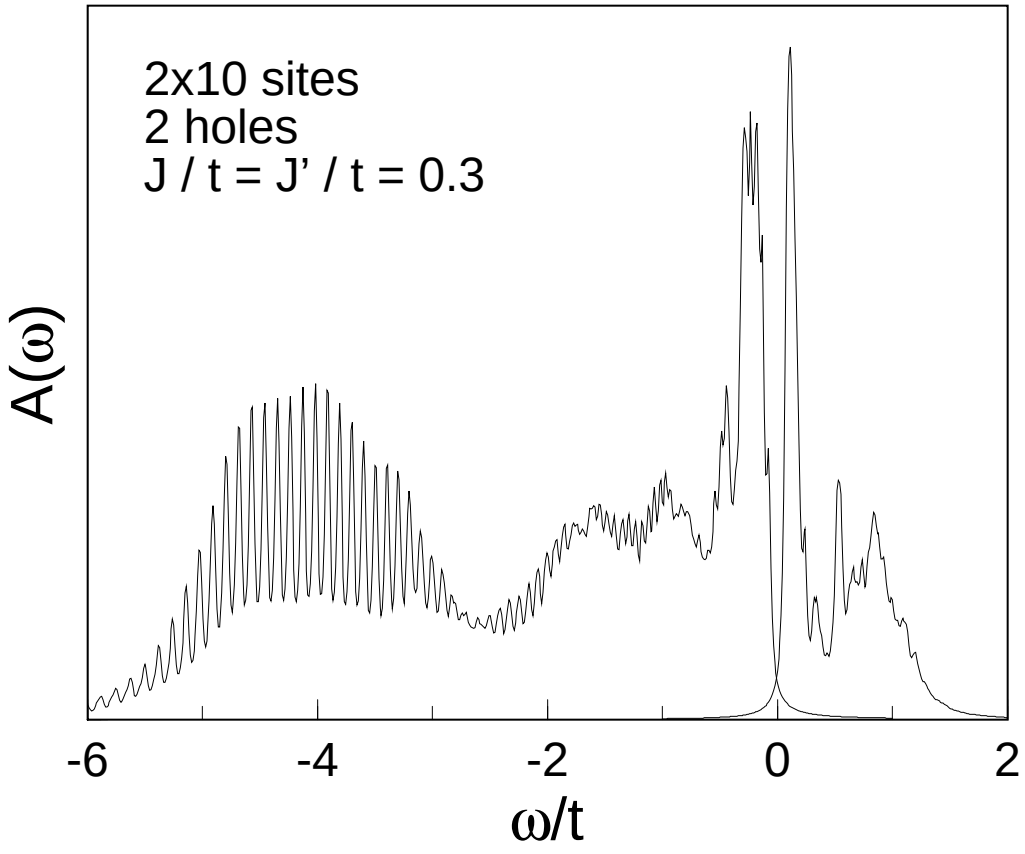
2x10 sites
2 holes
J / t = J' / t = 0.3
A(ω)
-6
-4
-2
0
2
ω/t

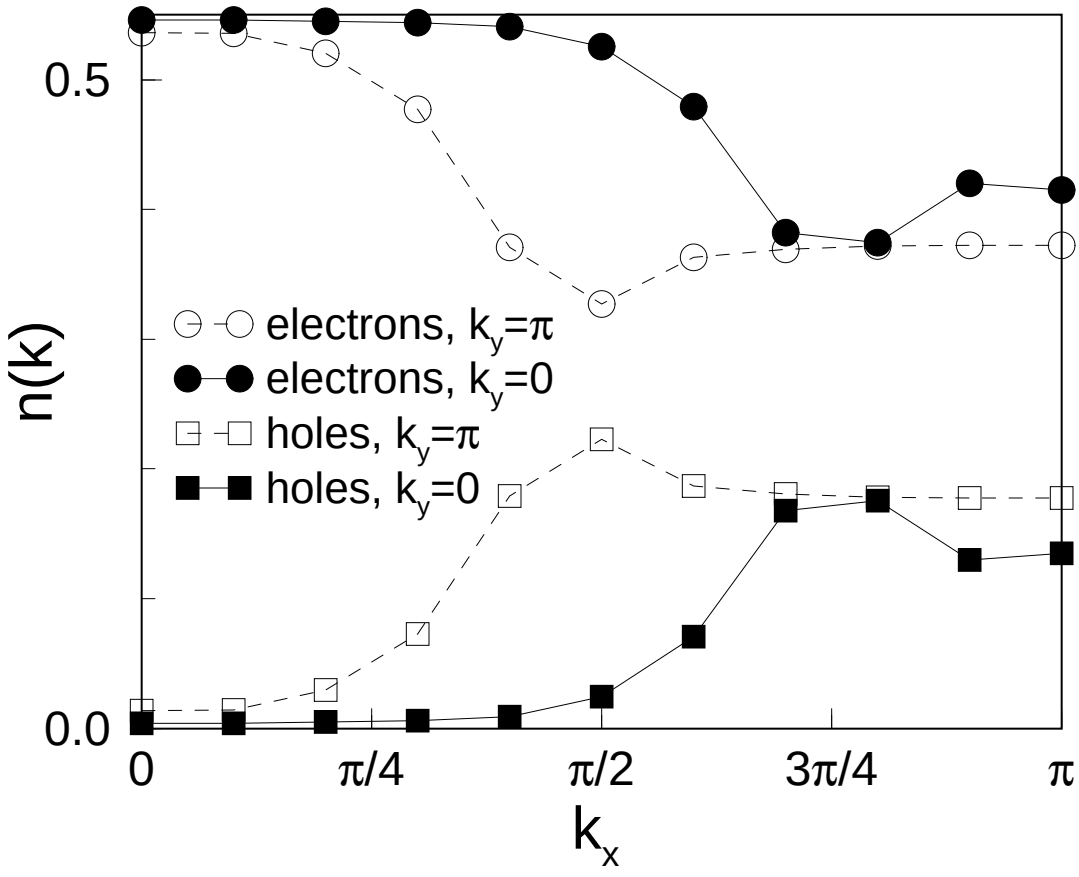
0.5
0.0
n(k)
electrons, k_y=π
electrons, k_y=0
holes, k_y=π
holes, k_y=0
0
π/4
π/2
3π/4
π
k_x